Linköping University | Division of Fluid and Mechatronic Systems
Master Thesis | Mechanical Engineering
Spring 2020 | LIU-IEI-TEK-A–20/03690—SE

A Novel Pump-Controlled Asymmetric Cylinder with Electric Regeneration

- Implementation and Evaluation of a Closed Hydraulic System on a Backhoe

---

Emil Fernlund

Supervisors:
Samuel Kärnell
IEI, Linköping University
Fabian Lagerstedt
Huddig AB

Examiner:
Liselott Ericson
IEI, Linköping University

Linköping University
SE-581 83 Linköping
013-28 10 00, www.liu.se

Abstract

The desire to use more energy efficient heavy equipment in the earth-moving industry has rapidly increased due to higher environmental awareness. Studies within electrification and new types of hydraulic circuit architecture has shown great potential regarding energy savings. The advantages of implementing a closed, pump-controlled, hydraulic system for controlling the boom cylinder on the backhoe of an articulated backhoe loader is evaluated in this thesis. The possibilities of electric energy regeneration is investigated and to what extent energy savings can be expected for the complete hydraulic system during normal operation.

In order for pump-controlled systems to even be conceivable alternatives to conventional valve-controlled system, they must be able to achieve the same characteristics and driveability as the original valve-controlled systems. The possibilities of imitating the characteristics of a valve-controlled hydraulic system with hydro-mechanical pressure feedback is also investigated in this thesis.

The original characteristic is able to be imitated with the implemented pump-controlled system with simple means by defining the current characteristic as the relationship between the operator input, cylinder load and cylinder flow. The evaluated sectioned hydraulic system demonstrates energy savings of 30 % during both a light and a heavy duty cycle. With components more suitable for this type of system and an improved control strategy, energy savings of over 50 % compared to the original system is believed to be possible.

Acknowledgments

This master thesis project has been a very educational, interesting and rewarding project. To be able to apply all knowledge gained from Linköping University into a practical and applicable area has tested my engineering skills and prepared me for future challenges.

I would therefore like to thank Huddig, HHK and Linköping University for this opportunity to do my master thesis within this innovative and fascinating field. I am particularly thankful of all the assistance from my supervisors, Samuel Kärnell and Fabian Lagerstedt, who has helped me throughout the whole project. Thanks for answering all my questions, even late at night, and all the interesting and helpful conversations. I would also like to thank all the help I received from the people at the R&D department at Huddig, no one mentioned, no one forgotten.

Finally, I would like to thank my girlfriend, Veronica, for always being there for me, through both fun and tough times. This work would not have been possible without your support and love.

Hudiksvall, June 2020
Emil Fernlund

Contents

Nomenclature

Acronyms

CoG	Center of Gravity	
EMC	Electric Motor Controller	
EMG	Electric Motor Generator	
HHK	Hudiksvalls Hydraulics Cluster	
ICE	Internal Combustion Engine	
LiU	Linköping University	
PRV	Pressure Relief Valve	

Symbols

Δp	Pressure difference	Pa
$\eta_{vol,b}$	Efficiency, volumetric boost pump	%
$\eta_{vol,p}$	Efficiency, volumetric main pump	%
ρ	Density	kg/m^3
ε	Displacement setting	–
A_{cA}	Piston area, chamber A	m^2
A_{cB}	Piston area, chamber B	m^2
C_q	Orifice flow coefficient	–
D	Displacement, main pump	cm^3
D_b	Displacement, boost pump	cm^3
E	Energy	J
F_{load}	Load force	N
F_{mg}	Gravitational force	N

g	Gravitational acceleration	m/s^2
h_{CoG}	Height of CoG	m
I	DC current	A
m	Mass	kg
n	Rotational speed	rpm
p	Pressure	Pa
p_{cA}	Cylinder pressure, chamber A	Pa
p_{cB}	Cylinder pressure, chamber B	Pa
p_{pA}	Pump pressure, port A	Pa
P_{bat}	Battery power	W
P_{cyl}	Cylinder power	W
P_{pot}	Potential power	W
P_p	Pump power	W
q	Flow	m^3/s
$q_{\Delta A}$	Area compensating flow	m^3/s
q_{cA}	Cylinder flow, chamber A	m^3/s
q_{cB}	Cylinder flow, chamber B	m^3/s
s	Stroke length	m
t	Time	s
U	DC voltage	V
v_{cyl}	Cylinder speed	m/s
$v_{v,CoG}$	Vertical speed of CoG	m/s

Chapter 1

Introduction

This chapter will give an insight of the master thesis conducted at Huddig AB. The background to this project as well as its aim, objectives and delimitations are presented below.

1.1 Background

With the higher environmental awareness and the human affect on the environment the desire for energy efficiency rapidly increases. This applies to all sectors in society, the food industry, energy production, transportation and manufacturing among others. The growing population and higher standards of living, put pressure on the different sectors to become more energy efficient and to reduce material waste in order to be more environmentally friendly. These are some big challenges the society has to face. To solve these, we "...need new ideas, new innovations and more large-scale failures than ever"[1].

These challenges have resulted in several research collaborations, one being STEALTH (Sustainable Electrified Load Handling). STEALTH is a collaboration between Hudiksvalls Hydraulics Cluster (HHK) and Linköping University (LiU), and has the purpose to investigate the possibilities of electrification and minimising the energy consumption of load handling machines and earth-moving machinery. A part of the collaboration includes building and evaluating three demonstrators, two load handling cranes and one backhoe loader.

This thesis will handle the demonstrator on the backhoe loader. The demonstrator in detail is a subsystem of the complete hydraulic system and is developed to control the boom cylinder on one of Huddigs diesel-electric hybrids called Tigon.

1.2 Aim and Objectives

The aim for this thesis is to investigate and evaluate a closed hydraulic system for the boom cylinder on the backhoe with the purpose of being more energy efficient and be able to regenerate energy when lowering the boom.

One of the most important features of a Huddig backhoe loader is the characteristics and driveability. The first objective is thus to analyse and define the current characteristics of the backhoe boom on the Tigon. The second objective is to maintain these attributes when completely changing the conventional hydraulic system into a closed, electric and pump-controlled, hydraulic system. The third objective is to make an energy analysis of the new boom cylinder system and the ability to regenerate energy. The last objective is to compare the energy usage for the complete new system with the original.

1.2.1 Research Questions

In order to achieve the objectives described above, the following questions should be answered:

- How can the existing characteristics of the backhoe be measured and defined?
- How can a similar characteristic of the backhoe with the new system be achieved?
- To what extent is it possible to regenerate energy from the boom cylinder on a backhoe?
- How much energy savings can be expected with the new system compared to the original system?
- Are the chosen components suitable for this type of system or how can they be improved or replaced?

1.3 Delimitations

During investigations and evaluations of a new hydraulic system, there are a lot which can be taken into consideration. Since this is a first study on this kind of system on a Huddig machine, no optimisation of the components and control strategy is evaluated. The project is estimated to be completed within 20 weeks, which limits the depth of the investigations, and as such, several delimitations have been set.

- The components for the new system has not been implemented on the actual machine, it was built as an external rig and only connected to the machine through hydraulic hoses and CAN communication.
- The boom slew and side angling functions was not used during any of the analysis of the backhoe.
- The used components was chosen in advance by Huddig and were very limited for change.
- The energy analysis is based on two different load cases.
- The focus was not on the control strategy for the new boom cylinder system.

1.4 Outline

Chapter 1 initiates this thesis by describing the background and aim for this project. It also describes the main objectives and the research questions that the thesis will give answers to. After the introduction follows Chapter 2, where related research and different approaches to pump-controlled systems are described. The Tigon and the backhoe is presented in Chapter 3, together with the original and new hydraulic system. The components in the new hydraulic system is all described in Chapter 4, together with a description for how the Tigon communicates with the external rig. The characteristic of the backhoe is defined and measured in Chapter 5. The used strategy for the new system to achieve this characteristic, and the resulting characteristic is also presented in Chapter 5. Chapter 6 presents how the characteristics of the original system is used in the control strategy for the new pump-controlled system. Further, how the rotational speed and displacement setting is chosen in each operating point. The new pump-controlled system is analysed regarding energy efficiency and regeneration capacity in Chapter 7. The energy usage for the complete backhoe for the original and new system is also analysed in this chapter. The rig, the chosen components, the resulted characteristics and the results from the energy measurements are discussed in Chapter 8. The final chapter, Chapter 9, answers the research questions, proposes some future work and summarises the thesis.

Chapter 2

Related Research

As an introduction to the thesis this chapter will bring clarity to relevant research and different approaches for controlling pump-controlled asymmetric cylinders.

2.1 Pump-Controlled Systems

Pump-controlled systems has been a research topic since the late 1980s with a focus on energy efficiency and compensating for the differential flow due to asymmetric cylinders. Although it has been a research topic for a long time, the technology has not yet had its industrial breakthrough [2]. The importance of the efficiency of hydraulic systems has become a concern and the interest in pump-controlled systems has increased in recent years due to the desire to reduce the human impact on the environment. In heavy machinery, including earth moving and load-handling machines, valve-controlled systems are commonly used. Since these systems introduces unwanted throttling losses, pump-controlled systems is thought to be a possible solution to increase the system efficiency [3], [4]. So, instead of controlling the flow with valves, pump-controlled systems, as the name indicates, controls the flow to the actuators directly from the pump.

The hydraulic circuit design of pump-controlled systems are often divided into two types; open and closed circuits, illustrated by Figure 2.1. These two types only refers to the design of the hydraulic circuit architecture and if the pump can pressurise only one or both pump ports. How the flow is controlled and how the differential flow is compensated for introduces many different solutions and control strategies for pump-controlled systems.

Due to the many types of pump-controlled systems, [2] has classified and reviewed different pump-controlled cylinder drives. The classification is divided into three different parts, the *Hydraulic Supply Classification*, *Circuit Architecture* and *Flow Compensation Method*. The *Hydraulic Supply Classification* describes if the system uses one or two prime movers and one or multiple hydraulic pumps. Also, if these pumps control the flow with variable speed and fixed displacement, fixed speed and variable displacement or both variable speed and variable displacement. The last class is however not included in the review in this publication. The next

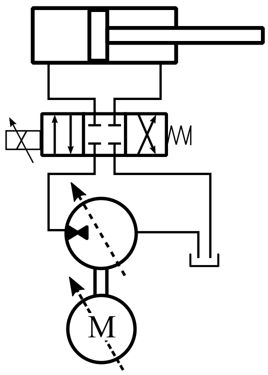

(a) Schematic circuit of a open pump-controlled system. Only one of the pumps ports can be pressurised.

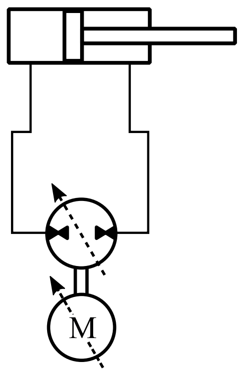

(b) Schematic circuit of a closed pump-controlled system, also know as direct drive. Both ports on the pump can be pressurised.

Figure 2.1: Schematic circuit of a open and closed pump-controlled system.

step in the classification is the *Circuit Architecture*, if it is an open or closed hydraulic circuit, as described in Figure 2.1. The last step is the *Flow Compensation Method* which, for example, includes *Active valves*, *Passive valves* or a *Asymmetric Pump*. In a comparison between the classes described above, [2] presents that systems using variable speed and fixed displacement pumps has higher efficiency, better compactness and flexibility, and has a simpler hydraulic circuit compared to systems with variable displacement and constant speed. The latter does, however, have higher reliability, are easier to scale and have a higher ability to control drive stiffness. The efficiency is, however, significantly improved for all classes compared to conventional valve-controlled systems, but during part load the classes with variable speed achieves higher efficiency.

A conclusion made in multiple publications is that the energy efficiency can be greatly improved with pump-controlled systems compared to conventional valve-controlled systems [2], [5], [6]. How large this energy efficiency increase is, depends on the specific application, the chosen components and the hydraulic architecture. In [2] it is concluded that significant energy savings are possible, up to 75 % for certain types of pump-controlled circuits compared to separate metering valve-controlled systems.

The main drawback with pump-controlled systems has been the dynamic behaviour, since there are no throttling losses there are no introduced damping in the system [7]. To accomplish better dynamic behaviour, the control strategy is significant for pump-controlled systems, regardless of if the system is controlled by variable speed, variable displacement or both. During the latest years improvement on electric motors an increased response and controllability of pump-controlled systems with variable speed has been made possible. The dynamic behaviour of pump-controlled systems is however still a research area that needs future focus [8].

2.2 Flow Compensation

In closed hydraulic systems, the difference between the flow into and out of the asymmetric cylinder must be compensated for. As mentioned, [2] goes through a variety of different solutions for this problem. Pilot operated check valves and an accumulator is used in [4], where the dynamic behaviour is investigated with good results. Instead of the accumulator, [9] uses an external charge circuit that provides extra or drains excess flow. There are several other different approaches to compensate for the differential flow, for example the use of passively actuated directional valves or a hydraulic transformer are also some of the classes reviewed in [2]. These different types are of different complexity and efficiency, and are best suited for different types of applications.

2.3 Control Strategies

Early pump-controlled systems in mobile application were often controlled by variable displacement pumps with an internal combustion engines (ICE) as prime mover. With the current available hydraulic pumps on the market, pumps with variable displacement often have a lower efficiency at low displacement settings compared to at full displacement or fixed displacement pumps. With the improved efficiency and controllability of electric motors, speed-controlled systems have been investigated in multiple applications during the last years [10].

With the demand for energy efficiency and electric drive within the mobile applications sector, research on speed-controlled hydraulic systems has rapidly increased. Speed-controlled systems, however, suffer from higher starting torque and vibrations with higher amplitudes at low flow rates. Variable speed pumps also has variable resonant frequencies which is more difficult to suppress than the frequencies from constant speed systems. But by using pumps with more cylinders, the starting torque and the vibrations are reduces, it however increases the complexity of the pump.

In order to investigate the possibilities of utilising the advantages of both displacement and speed controlled systems, studies have been conducted on this type of system. By introducing a second control variable, the control strategy can be used to optimise the rotational speed and displacement setting regarding to energy efficiency or system dynamics [8]. According to [3] and [8] a speed and displacement controlled system has the potential to reduce the energy consumption by at least 20 % compared to pure speed or pure displacement controlled systems. A novel process-adapted control concept is presented in [8]. This control concept uses a mathematical optimisation model to minimise the energy consumption for a system with two degrees of freedom, here the rotational speed and the displacement setting. It is also concluded in [8] that speed- and displacement-variable pumps can double the volume flow gradient, which can be utilised to improve the dynamic behavior of pump-controlled systems. A different approach is to investigate the behaviour of a system at the transition between the different quadrants presented in Section 2.4, [4]. A hydraulic circuit and control strategy that instead enhances the response in the transition area is proposed. This strategy reduces system oscillations in the transitions, however with the cost of an increased energy consumption. The control strategy is thus of great importance in systems with multiple degrees of freedom, and there is no optimal strategy for all different systems and applications but is dependent on the desired optimisation goal.

2.4 Four Quadrant Drive

To benefit from all advantages of a pump-controlled closed hydraulic system, it must be able to handle all possible scenarios for the cylinder. Since the external load can act in two directions, and the desired motion of the cylinder can also be in two directions, the four different scenarios are established, also known as *the four quadrants*, illustrated in Figure 2.2. Quadrant 1 is defined for positive flow with a counteracting load. If the load changes direction and acts together with the desired motion, the hydraulic machine acts as a motor, this scenario is defined as quadrant 4. The same applies for quadrant 2, but with the direction of both the load and desired motion inverted. Quadrant 3 is thus the same as quadrant 1, but also with the direction of both the load and desired motion inverted.

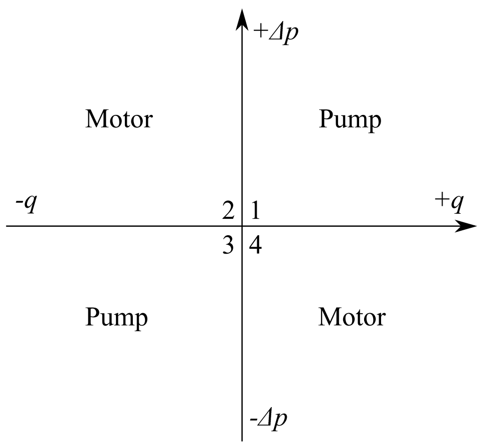

Figure 2.2: The four quadrants that a direct driven hydraulic system can operate in.

Chapter 3

System Description

This chapter provides an overview of the machine, the original and the new hydraulic system. Also, some advantages with the new system are briefly explained.

3.1 Backhoe

The investigated machine is the Huddig Tigon concept machine in Figure 3.1, which is a articulated backhoe loader. The Huddig machine has no specific area of use. The main advantages according to owners and operators are the versatility and flexibility [11]. It is a wheel loader, excavator and maintenance machine all in one. It has better accessibility in difficult terrain than an excavator, it can have equipment mounted both in the front loader and on the backhoe. It can be mounted with rail wheels and a lift to do maintenance work on train rails, overhead power lines and road lighting among others.

Figure 3.1: Huddig Tigon concept machine. Courtesy of Huddig.

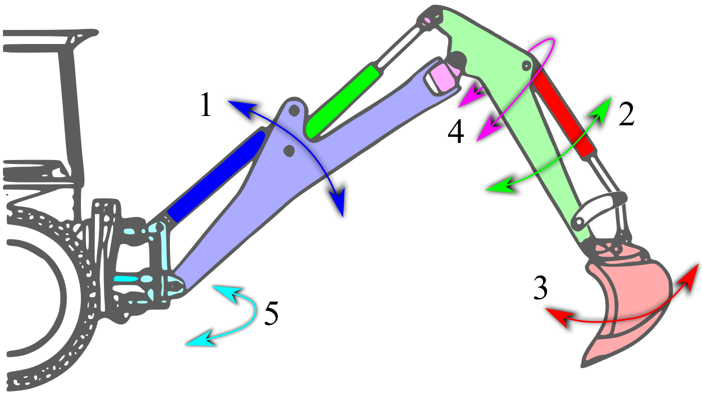

Figure 3.2: Backhoe with the standard five functionalities. (1) Boom, (2) Dipper, (3) Bucket, (4) Side angling, (5) Boom slew.

The backhoe on the Tigon, Figure 3.2, has five standard functionalities, boom, dipper, bucket, side angling and boom slew. Huddig has previously made measurements and found that the largest power consumer in the backhoe is the boom cylinder. The boom cylinder has also been found to have the highest potential regarding energy regeneration. The test rig will therefore be implemented on this cylinder to minimise the power consumption and investigate the extent of energy regeneration. Since the cylinder stroke position for the dipper and bucket affects the Center of Gravity (CoG) on the backhoe and therefore the force on the boom cylinder, these positions has to be taken into account during the analysis of the boom cylinder. However, to reduce the complexity of the backhoe but maintain functions affected by gravity the side angling and boom slew is not used during the energy analysis. By removing the slew and side angling the backhoe mechanics can be simplified from a 3D problem into a 2D problem.

3.2 Original System

The hydraulic actuators on a backhoe loader or excavator has traditionally been powered by the ICE, which usually is a diesel engine. The ICE powers a single hydraulic pump, or a pump group, which supplies flow and pressure to all the actuators through a variety of slide valves in a valve manifold, as illustrated in Figure 3.3. The ICE rotates with a constant speed, and the flow into the valve manifold is controlled by the displacement setting of the hydraulic pump.

To improve the energy efficiency of a conventional Huddig machine, an extra prime mover hos been added to power the hydraulic system on the Tigon, hereafter referred to as the *original system*. Electric propulsion and some other improvements have also been implemented on the Tigon, but none of these improvements are in the focus of this report. The added components for the hydraulic system is a battery, a Electric Motor Controller (EMC) and a Electric Motor Generator (EMG), as illustrated in Figure 3.4. A clutch has also been implemented between

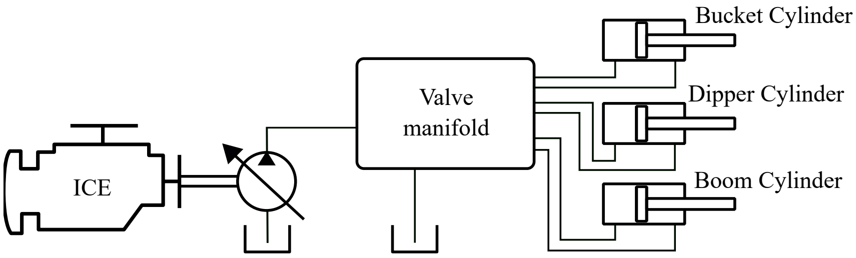

Figure 3.3: Conventional system with ICE, variable displacement pump, valve manifold and the three used cylinders.

the ICE and the hydraulic machine to be able to decouple and turn off the ICE. If the ICE is turned off and decoupled from the hydraulic system, the EMG is used as the rotational power source. If the battery charge status is low, the ICE is turned on and the EMG runs as generator to recharge the battery.

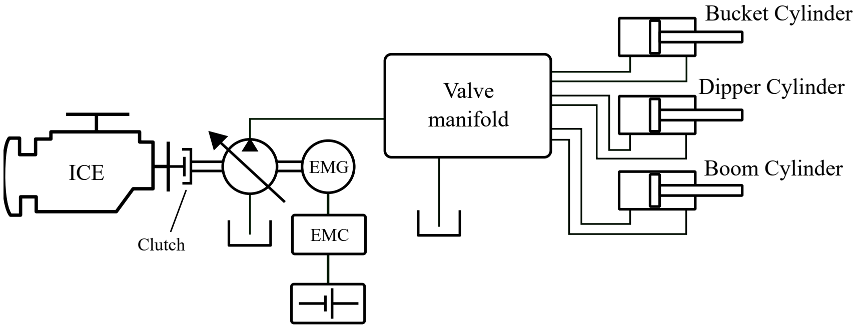

Figure 3.4: Original system on the Tigon machine.

The hydraulic system utilises load sensing technology to minimise the hydraulic losses. However, the losses can still be of great magnitude if the pressure difference between multiple moving cylinders is substantial. The boom cylinder can for example have a high load, the dipper cylinder a smaller load and the bucket cylinder an even smaller load, as illustrated by the pressure/flow diagram in Figure 3.5. Since the pump, or pump group, needs to provide the requested flow at the highest required pressure, illustrated by the operation point, the throttling losses for cylinder 2 and 3 can be extensive. One way of minimising these losses is to split up the hydraulic system into multiple systems. This means that the pressure can be adapted to better fit the demanded pressure, and large parts of the throttling losses can be reduced.

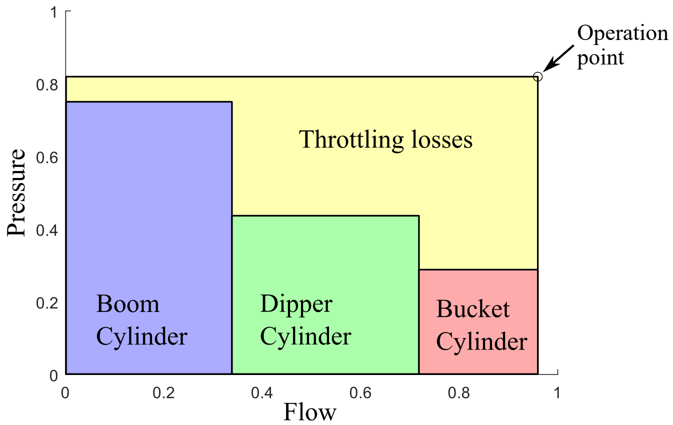

Figure 3.5: Load distribution and losses, original system.

3.3 New System

As described in Section 1.2, the aim is to use a decoupled system for the boom cylinder to be able to increase the energy efficiency and be able to regenerate energy when lowering the boom. This implies that the boom cylinder system will have its own EMC, EMG and hydraulic machine which is illustrated in Figure 3.6. All components in the *New boom cylinder system*, except the actual boom cylinder, will hereafter be referred to as the *rig*. The rig also has its own battery and oil reservoir for easier implementation on the machine. The components in Figure 3.6 that are not included in the *New boom cylinder system*, i.e. the components controlling the Dipper and Bucket Cylinder, will hereafter be referred to as *components on the Tigon*, or simply *Tigon*, when referring to the new system.

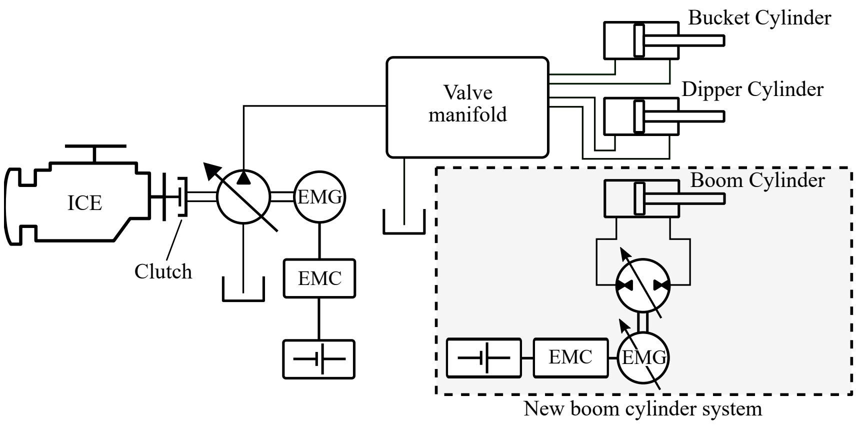

Figure 3.6: The new hydraulic system, with components indicated for controlling the boom cylinder.

Since the new system for the boom is a closed, pump-controlled system, and the cylinder is of single rod type with asymmetric areas, the flow difference between the two cylinder chambers must be handled. There are many different solutions to this problem, and [6] goes through several of them. One solution is to use accumulators to store the excess oil when needed [12], another solution uses a low pressure boost pump, check valves and a dump valve to add or drain excessive oil when needed. The latter is used in this system, and the hydraulic circuit is presented in Figure 3.7. All main hydraulic components are described in Section 4.2, in the next chapter. Since [2] does not include variable speed and variable displacement systems in the classification, the system used in this thesis is not directly comparable to any of the reviewed systems. The used system is a combination of the *Variable-Speed Single Prime Mover with Multiple Pumps* and *Single Constant-Speed Prime Mover and Multiple Pumps* systems in [2], also referred to as *B2* and *D2*, since it uses one prime mover, multiple pumps, the main and boost pump, and has both variable speed and displacement.

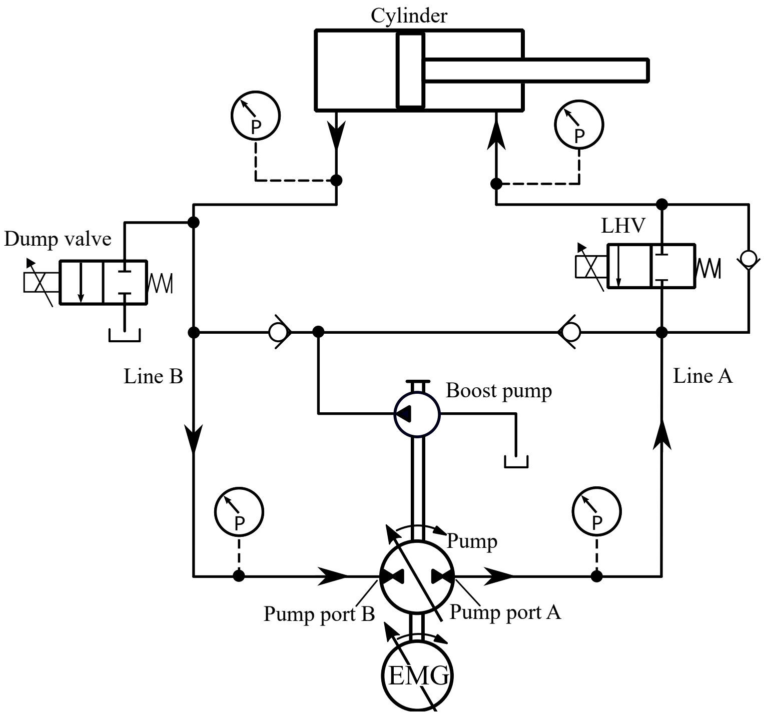

Figure 3.7: Schematic illustration of the hydraulic circuit of the new system for the boom cylinder. Positive flow is indicated by the arrows in the figure.

The flow direction in the rig during the four quadrants explained in Section 2.4 are presented in Figure 3.8. The hydraulic machine operates as a pump in quadrant 1 and 3 and as a motor in quadrant 2 and 4. Quadrant 4 is however not an functional case. With a negative load and a desired positive flow direction, i.e.

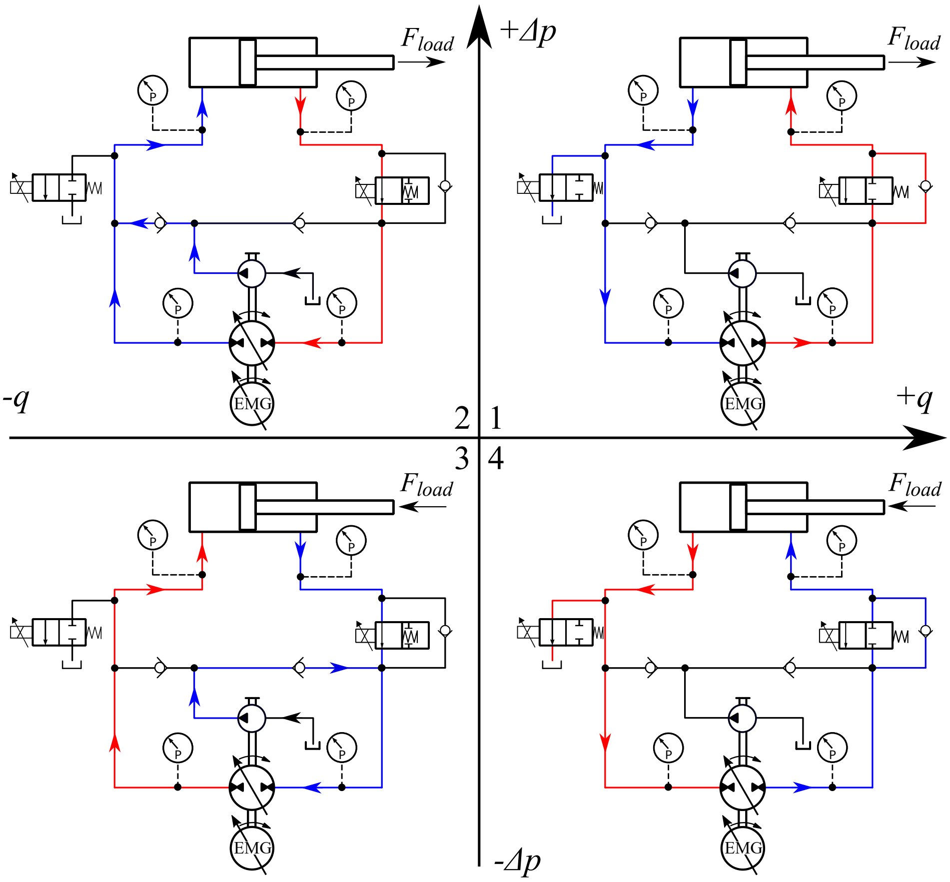

Figure 3.8: Illustration of the direction of the flow during operations in the different quadrants. High pressure represented by red line and boost pressure by blue line.

retraction of the cylinder, the dump valve is opened to eliminate the excess oil reducing the pressure in the B line to the boost pressure. With the reduced pressure the pressure difference changes from negative to positive and the operation has changed to quadrant 1. The rig can thus only regenerate during extension of the cylinder and a positive load force, i.e. quadrant 2.

With the implemented new system for the boom cylinder the complete hydraulic system is sectioned into two separate systems. This entails the possibility of having two different operating points, one for each part of the system. Which consequently means that the throttling losses in Figure 3.5 can be reduced to the losses in Figure 3.9. The extra losses for the original system occurs due to differences in load pressure. By dividing the original system into multiple systems, losses can be reduced. The number of parts in the system is however increased which results in a more expensive system.

The new boom cylinder system, built as an external rig, is shown in Figure 3.10.

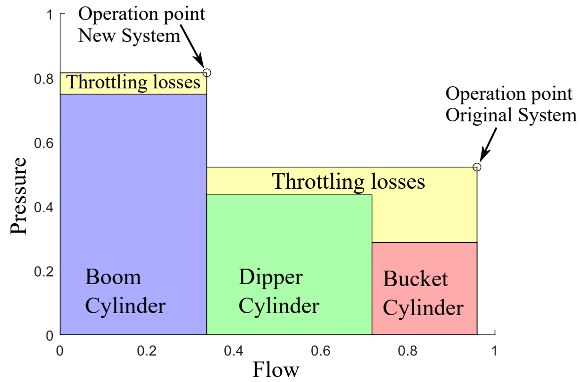

Figure 3.9: Load distribution and losses, new system.

The used components of the rig and how they communicate are described in Chapter 4.

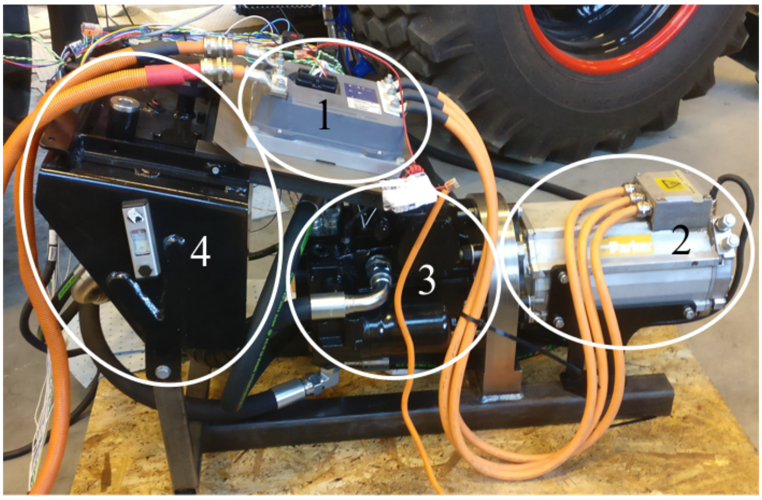

Figure 3.10: The rig with the main components used for controlling the boom cylinder. 1. EMC, 2. EMG, 3. Hydraulic machine, 4. Oil reservoir

Chapter 4

System Components and Communication

The components were all chosen in advance by Huddig, this chapter is only intended to give an insight into the functionalities of the components and how they interact with each other. The system for the boom cylinder is divided into two separate parts. The first part handles the conversion from chemical power in the battery to rotational power on the shaft between the electric machine and the hydraulic machine. The second part converts the rotational power to linear power through the hydraulic machine and cylinder.

4.1 Electric System Components

This section is only intended as a presentation of the used electrical power components and will not give detailed information on how they operate. The electrical power system includes a battery, a EMC and a EMG, illustrated in Figure 4.1. The used energy storage device is a lithium iron phosphate battery. The electric machine is used as both a motor and generator, thus giving it the name Electric

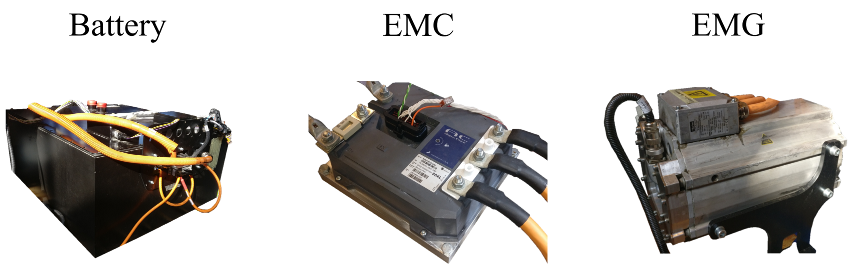

Figure 4.1: Electric system components.

Table 4.1: Used data for the EMG, [13].

Description	Value
Maximum rotational speed	2000 rpm
Rated torque	185 Nm

Motor Generator. The used EMG is a Parker GVM210, with the data presented in Table 4.1. The EMG is of type permanent magnet, three phase, alternating current with the advantages of having high efficiency and the ability to maintain high torque at low speeds [14]. The EMG is controlled by an InMotion ACS GEN6 motor controller, with a internal control loop for controlling the speed, n, of the EMG depending on the reference signal n_{ref}, illustrated by Figure 4.2.

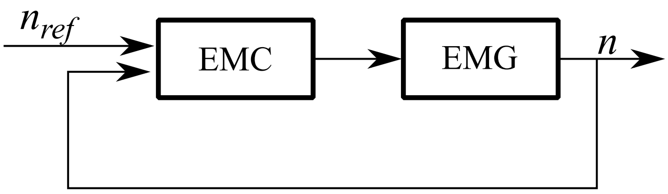

Figure 4.2: EMG feedback control system.

4.2 Hydraulic System Components

The hydraulic components converts the rotational power from the EMG into linear power out from the cylinder, or vice versa. For safety reasons, two shock valves are implemented to limit the maximum pressure in the new boom cylinder system, illustrated in Figure 4.3. Other essential components is the cylinder and the load holding valve, (LHV), which is mounted directly on the backhoe.

4.2.1 Hydraulic Machine

The purpose of a hydraulic machine, is to either convert rotational speed and torque into hydraulic pressure and flow, or vice versa. The machine can be of various type, for example gear machine, axial piston machine or radial piston machine. For more details about hydraulic machines see [15]. A hydraulic machine can act as a pump, a motor, or both. If the hydraulic machine can act as both a pump and motor depends on the design of the machine. The used hydraulic machine is designed to operate as a pump, it can however be used as a motor, but with reduced efficiency. The mode of operation depends on the surrounding circumstances and the desired rotational direction. The hydraulic machine will hereafter be referred to as pump.

The pump used in this project is an axial piston machine, of swash plate type, with variable displacement. See Figure 4.4 for a section view of the pump, with a

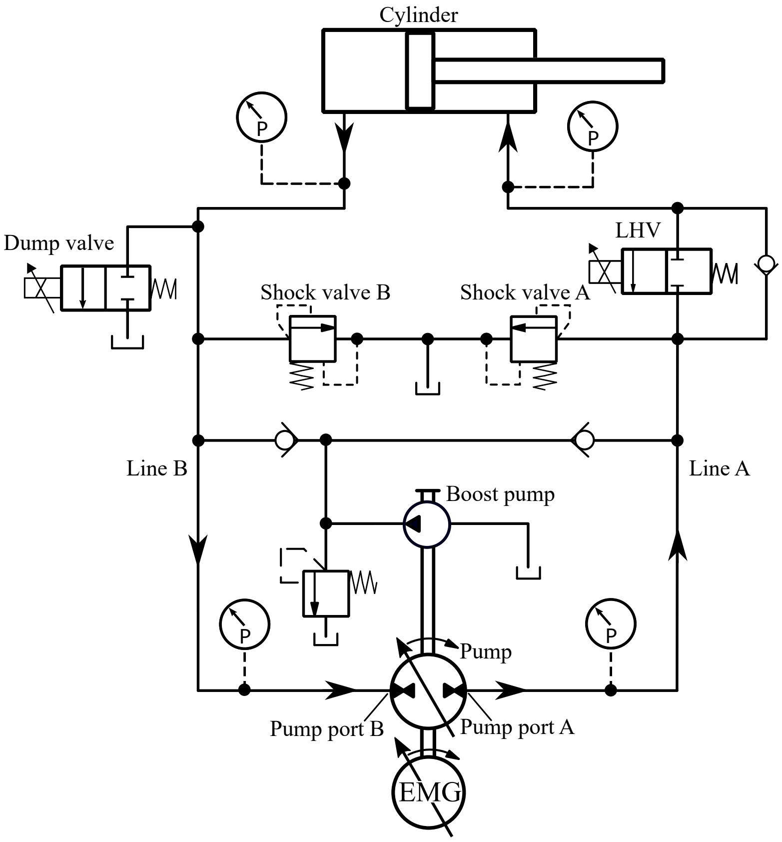

Figure 4.3: Complete circuit of the hydraulic system.

description of the internal parts.

The displacement setting of the pump is continuously variable between −1 and +1. It can thus have full displacement in both directions. The displacement is changed via the *Stroking piston*, which is controlled by the *Control unit*, which for the used pump is a displacement setting valve, illustrated in Figure 4.5. This valve is controlled electronically and is pressurised from the *Boost pump*. The displacement control is thus relying on the pressure from the boost pump, which in turn depends on the speed of rotation. The pump must rotate at a speed of at least 500 rpm to supply sufficient pressure to the displacement setting valve. The ratio between the main and boost pumps displacement are important for the system implementation and will be described why in Section 4.2.1. The displacement of the two pumps and rotational speed limitations are presented in Table 4.2. The complete hydraulic circuit for the pump is presented in Figure 4.5 with the main components specified.

The proposed hydraulic system for the rig utilises a boost pump and two check valves, as described in Section 3.3, to feed the necessary flow into the system to

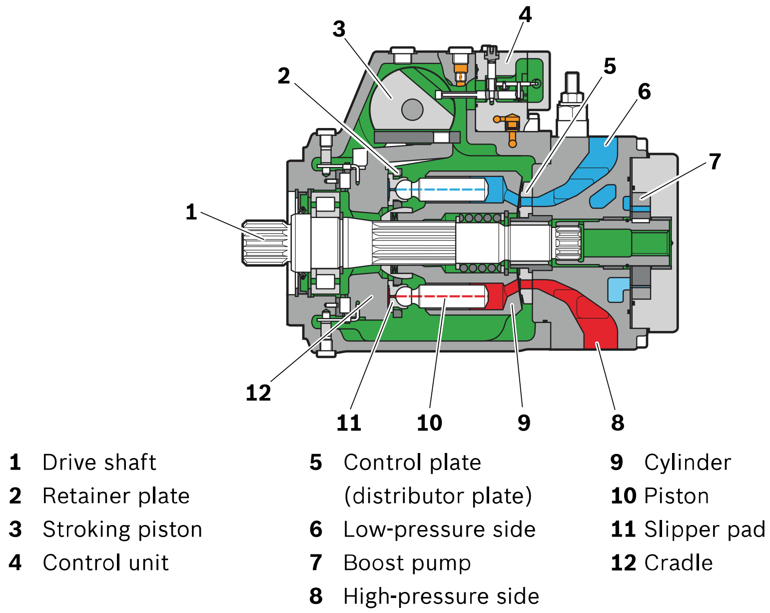

Figure 4.4: Section view of a swash plate axial piston pump [16], with description of internal parts.

Table 4.2: Data for the hydraulic machine [17].

Description	**Value**
Main pump displacement	125 $\mathrm{cm}^3/\mathrm{rev}$
Boost pump displacement	28.3 $\mathrm{cm}^3/\mathrm{rev}$
Minimum rotational speed	500 rpm
Maximum rotational speed	2850 rpm

compensate for the flow differences between the two chambers, hereafter referred to as the *area compensating flow*. The maximum feeding pressure from the pump is controlled with the *Pressure reducing feed valve* and is set to 210 bar. When the pressure reaches 210 bar the valve opens and reduces the pressure to the *displacement setting valve*, which reduces the displacement setting and thereby the flow and pressure. To limit the maximum pressure in the system a *shock valve* on each side of the pump are used. The shock valve on the A side is set to 250 bar and on the B side set to 175 bar. To minimise the risk of cavitation the boost pressure, and thus also the minimum pressure in the system is set by the *low pressure relief valve* to 25 bar.

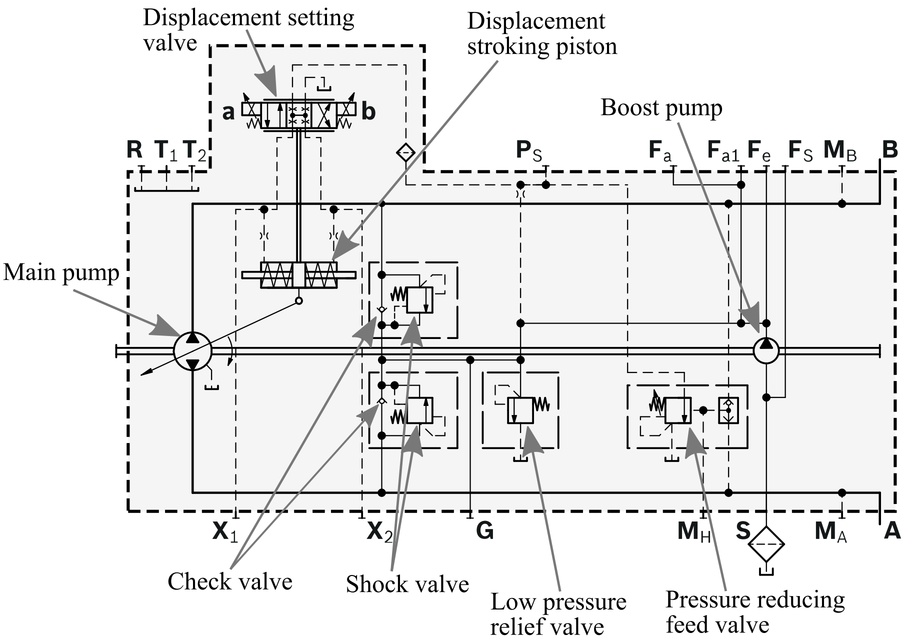

Figure 4.5: Complete circuit of the hydraulic machine [17].

Displacement Setting Limitations

As mentioned above, the volumetric differences in the cylinder chambers is either compensated by the integrated boost pump or the dump valve depending on if the cylinder is extending or retracting. The boost pump is utilised at positive stroke, i.e. extending, and the dump valve at negative stroke, i.e. retracting. During positive stroke, the flow from the boost pump can either go into line A or line B depending on which side is the low pressure side.

For the boost pump to be able to supply enough flow to compensate for the flow difference between cylinder chamber A and B the displacement setting on the main pump may have to be restricted. To calculate the maximum displacement setting for the main pump, the operation in quadrant 2 is first studied. Line B is the low pressure line and the pump is in this case in motor operation. The area compensating flow is supplied directly to the B line indicated by the red arrow in Figure 4.6.

To find the maximum displacement setting the cylinder chambers flow is described as

$$q_{cA} = v_{cyl} A_{cA} \tag{4.1}$$

$$q_{cB} = v_{cyl} A_{cB} \tag{4.2}$$

respectively. The difference between these two flows is the required flow from the boost pump, the so called *area compensation flow*, $q_{\Delta A}$. Since there is no added or drained flow in the A line, the flow through the pump is the same as

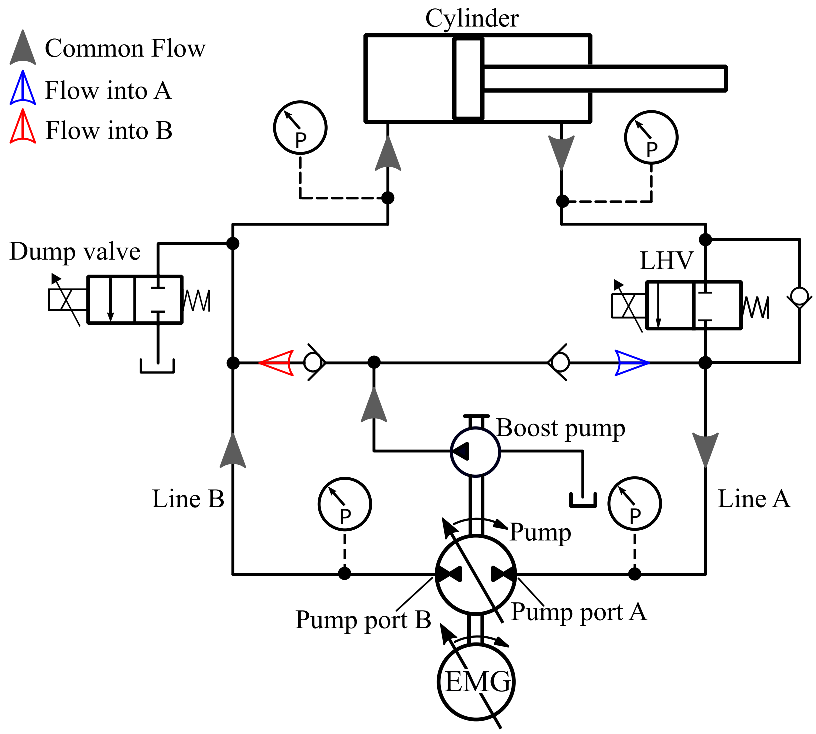

Figure 4.6: Hydraulic circuit and flow directions for the studied cases.

the flow out from chamber A, $q_{pA} = q_{cA}$. q_{cA} can thus be express in terms of rotational speed, n, main pump displacement, D_p, displacement setting, ε, and the volumetric efficiency of the pump, η_{vol}:

$$q_{cA} = nD_p\varepsilon \frac{1}{\eta_{vol,p}} \ . \tag{4.3}$$

The stroke velocity is given by combining Equations (4.1) and (4.3)

$$v_{cyl} = \frac{1}{A_{cA}} \frac{nD_p\varepsilon}{\eta_{vol,p}} \ . \tag{4.4}$$

As mentioned, the area compensating flow, $q_{\Delta A}$, is calculated as the difference between the two chamber flows,

$$q_{\Delta A} = q_{cB} - q_{cA} \ . \tag{4.5}$$

By substituting the chamber flows in Equation (4.5) with Equations (4.1) and (4.2) and replacing the stroke velocity with the result from Equation (4.4), the area compensating flow may be expressed as

$$q_{\Delta A} = \frac{A_{cB}}{A_{cA}} \frac{nD_p\varepsilon}{\eta_{vol,p}} - \frac{nD_p\varepsilon}{\eta_{vol,p}} = \frac{nD_p\varepsilon}{\eta_{vol,p}} \left(\frac{A_{cB}}{A_{cA}} - 1 \right) \ . \tag{4.6}$$

The maximum available area compensating flow is given by the rotational speed, displacement of the boost pump, and the volumetric efficiency,

$$q_{\Delta A,max} = nD_b\eta_{vol,b} \ . \tag{4.7}$$

By combining Equations (4.6) and (4.7), the maximum displacement setting for operation in quadrant 2 ε_{max} is given by

$$\varepsilon_{max,q2} = \frac{D_b}{D_p}\frac{1}{\dfrac{A_{cB}}{A_{cA}} - 1}\eta_{vol,b}\eta_{vol,p} \ . \tag{4.8}$$

Using the same approach, but replacing Equation (4.3) with

$$q_{cB} = nD_p\varepsilon\eta_{vol,p} \ , \tag{4.9}$$

the maximum displacement for operation in quadrant 3 can be calculated. The area compensating flow for operation in quadrant 3 is supplied into line A, as illustrated by the blue arrow in Figure 4.6. The maximum displacement for this operation case can thus be calculated accordingly:

$$\varepsilon_{max,q3} = \frac{D_b}{D_p}\frac{1}{1 - \dfrac{A_{cA}}{A_{cB}}}\frac{\eta_{vol,b}}{\eta_{vol,p}} \ . \tag{4.10}$$

If the calculated ε_{max} is larger than 1, there is no need to limit the displacement setting.

The maximum displacement setting depends on the volumetric efficiency of the main and boost pump, as seen in Equations (4.8) and (4.10). During normal operations for the first case, where the main pump operates as a motor, the combined efficiency $\eta_{vol,b}\eta_{vol,p}$ is assumed to be 75 % resulting in a maximum displacement setting, $\varepsilon_{max,q2}$, of 50.0 %. For the second case, where the pump operates as a pump, the maximum displacement setting, $\varepsilon_{max,q3}$, is calculated to 105.8 %. The maximum displacement setting is thus set to 50 % to ensure that the flow from the boost pump is sufficient in both quadrants.

4.2.2 Cylinder

The hydraulic component that performs the linear actuation is the cylinder. The cylinder contains of a housing, a piston and a rod, illustrated in Figure 4.7. Hydraulic oil is pressed into one of the cylinder chambers and applies a pressure on one side of the piston. An external force is acting on the rod, which can either be a pulling or pushing force. As visualised in Figure 4.7, the piston area in chamber B is larger than the piston area in chamber A due to the size of the cylinder rod. This entails that the amount of oil in the system will differ at different stroke positions.

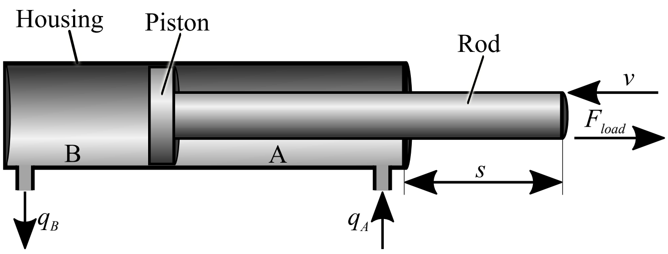

Figure 4.7: Section view of the boom cylinder. F_{load} and v indicate positive acting load force and stroke velocity. s is the current stroke position and q_A and q_B is positive flow direction. A and B represents chamber A and chamber B.

4.2.3 Valves

The new system is supposed to reduce as much losses as possible. Since valves introduces losses into the system, the use of valves are minimised. However, some valves are essential, both for safety reasons and to get a working system.

Load Holding Valve

The cylinder has a fitted LHV preattached to it. The use of LHVs is regulated by the International Organisation for Standardisation in [18] to minimise the risk of accidents during hose rupture or other accidents with pressure drop as a result. As illustrated in Figure 4.8, the flow during lifting goes through a check valve when going into the cylinder through port A1 on the LHV. During lowering of the boom, the flow must go through the controllable valve which is normally closed. If a hose rupture occurs, the controllable valve is used to hold, or safely lower, the boom to prevents accidents. The controllable valve is more complicated than shown in the figure, this is however not something that will be addressed in this thesis.

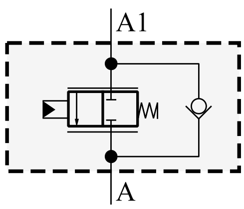

Figure 4.8: Circuit of the LHV. Port *A* is connected to port *A* on the pump, and the *A1* port is connected to the *A* port on the cylinder.

The check valve and controllable valve has different orifice areas and characteristics, the pressure drop across the valve is so forth different depending on the direction of the flow. If the flow goes into the cylinder, from port *A* to port *A1* in the LHV, the pressure drop is much lower than if the flow goes in the opposite direction, illustrated by Figure 4.9. However, since the characteristics is known, the losses in the LHV can be taken into account during the analysis of the system.

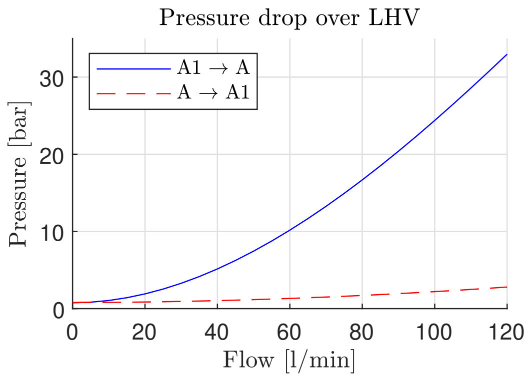

Figure 4.9: Pressure drop characteristic over the LHV for flows in the two different directions.

Dump valve

The dump valve actually consists of two valves as seen in Figure 4.10. A pressure relief valve, (PRV), and an On/Off valve. The On/Off valve is electronically controlled and opens if the pressure at the B port of the pump is higher than 27 bar during retraction of the cylinder. The PRV then regulates the pressure to the set boost pressure of 25 bar. If no PRV is used, the flow from cylinder chamber B and the boost pump would go directly to the tank resulting in a tank pressure at the B port of the pump and an increasing risk for cavitation in the pump. The PRV is thus used to limit the flow to tank and to maintain a minimum pressure of 25 bar at the B port of the pump.

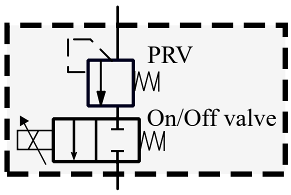

Figure 4.10: Dump valves with a pressure relief valve and a on/off valve.

Internal Pump Valves

The used pump also has multiple valves built into it, as seen in Figure 4.5. These valves are partly used as controlling valves for the pump, but also as safety valves for the system. The *Low pressure relief valve* is used to set the maximum pressure in the boost pump circuit. The *Pressure reducing feed valve* is used to limit the maximum output pressure from the main pump. The highest pressure from the main pump is sensed through the shuttle valve. If that pressure is higher than the preset pressure limit, the pressure reducing feed valve opens which reduces the pressure to the *Displacement setting valve* and thus reduces the displacement setting and consequently the pressure out from the pump. If the load of the backhoe increases over a predefined pressure one of the two *Shock valve*s opens and lets the flow into the boost pressure circuit and through the *Low pressure relief valve* into the oil reservoir. The two *Check valve*s are used to refill the main hydraulic circuit during extension of the boom cylinder.

4.3 Hydraulic Circuit

The complete hydraulic circuit, with the pump explained in Section 4.2.1, the cylinder in Section 4.2.2 and the valves in Section 4.2.3, is presented in Figure 4.11. The main difference from the circuit presented in Figure 4.3 is the chock valves, that here are integrated in the pump unit. As seen in the figure, the only hydraulic component needed in addition to what is already implemented on the Tigon is the hydraulic machine and the dump valve.

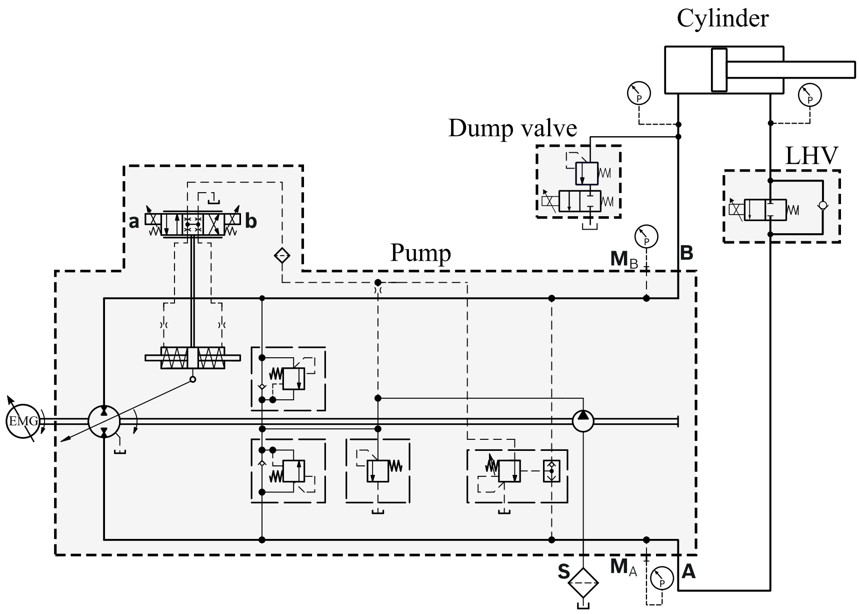

Figure 4.11: Complete hydraulic circuit for the new boom cylinder system.

4.4 Communication

The used components described in Sections 4.1 and 4.2 are illustrated with the communication circuit in Figure 4.12 and description in Table 4.3.

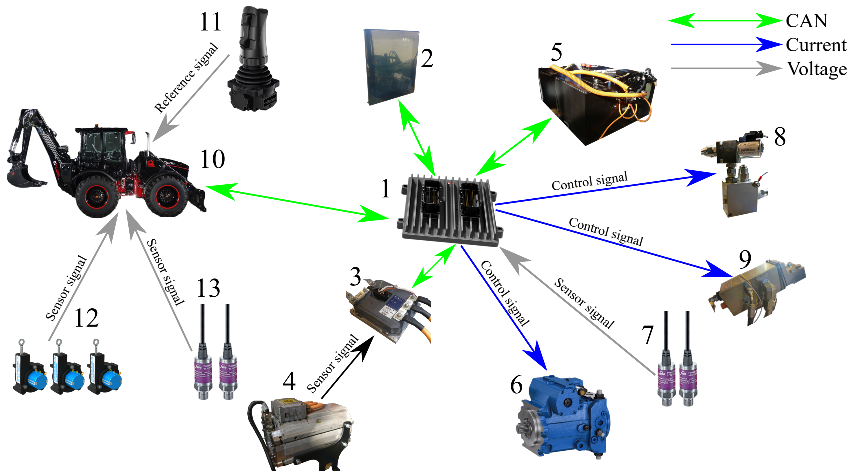

Figure 4.12: Circuit of the communication between all used components. The components are described in Table 4.3.

Table 4.3: Description of the components in Figure 4.12.

Number	Description
1	MC43FS, Master Controller
2	MD4, Master display
3	InMotion ACS GEN6, motor controller
4	Parker GVM210, EMG
5	Battery
6	Rexroth A4VG, hydraulic pump
7	Pressure transducer for port A and B on hydraulic pump
8	Dump Valve, on/off
9	Load Holding Valve
10	Huddig Tigon
11	Operator lever
12	Linear stroke transducers for boom, dipper and bucket cylinder
13	Pressure transducer for port A and B on boom cylinder

The master unit for controlling the rig is a Parker IQAN MC43FS, (1) in Figure 4.12. It has multiple CAN channels, voltage input channels and voltage, current and PWM output channels [19]. The control strategy implemented on the MC43FS is built using IQAN Design and is presented in detail in Chapter 6.

Three linear stroke transducers are attached to the three cylinders controlling the boom, dipper and bucket. Four pressure transducers, as displayed in Figure 3.7, is used to measure the pressures in different parts in the hydraulic system. The three stroke transducers and the two pressure transducers attached to the cylinder chambers are connected to the master unit on the Tigon machine and is broadcasted over CAN to the master unit on the rig together with the reference signal from the control lever, illustrated in Figure 4.12. The two pressure transducers connected to each side of the hydraulic pump are directly connected to the master unit on the rig.

Chapter 5

Characteristics

This chapter presents the used method to analyse the backhoe boom cylinder characteristics on the Huddig Tigon machine and how to achieve similar characteristics with the new hydraulic system.

5.1 Define Boom Cylinder Characteristics

To understand the characteristics of the backhoe boom cylinder, the current system is investigated. The Huddig machines uses a pressure feedback system to enable the operator to detect changes in force when maneuvering the backhoe. It is also used to damp the system and reduce oscillations. The pressure feedback reduces the flow to the cylinder where the pressure increases. The operator observes that a cylinder speed decreases and thereby knows that the force affecting that cylinder has increased. The pressure feedback system utilises the cylinder pressure to change the position of the spool valve, and thereby altering the opening area of the orifice, which then changes the flow to the cylinder. Not all functionalities of the backhoe has pressure feedback, on the boom cylinder the feedback system is only implemented during negative stroke, i.e. lifting the boom.

The flow through an orifice is a function of the orifice area and the pressure difference over the orifice, and is expressed as

$$q = C_q A \sqrt{\frac{2}{\rho} \Delta p} \; . \tag{5.1}$$

Due to the pressure feedback, the orifice area, A, is not only a function of the reference signal, r, from the operator, but also a function of the cylinder pressure, p_{cA}. This results in the following expression for the flow into cylinder chamber A

$$q_{cA} = C_q A(r, p_{cA}) \sqrt{\frac{2}{\rho} (p_{pA} - p_{cA})} \; . \tag{5.2}$$

Although, Equation (5.2) for the flow exists, it cannot be used to analyse the characteristics because it is unknown how the orifice area depends on the reference signal and the pressure feedback. Figure 5.1 illustrates however how the flow rate decreases for a heavier load for the same reference signal from the control lever. The characteristics of the boom cylinder is thus defined by the correlation

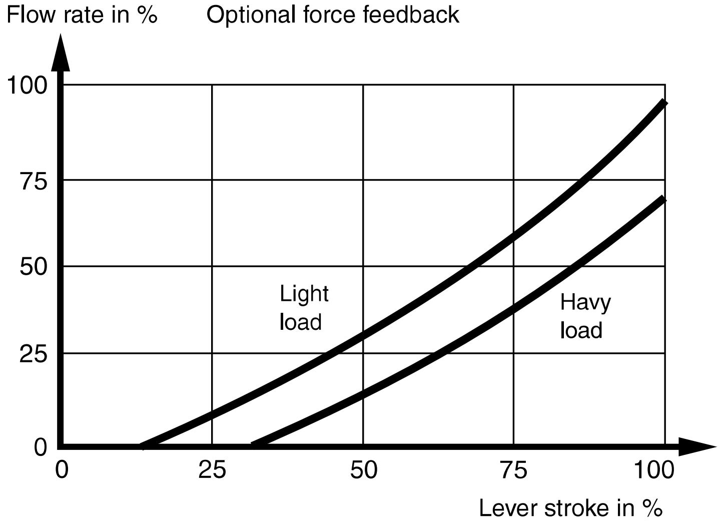

Figure 5.1: Schematic illustration of pressure feedback from Parker [20].

between operator reference signal, the pressures in the cylinder and the flow into the cylinder chambers.

5.2 Determine Boom Cylinder Characteristics

To determine the characteristics of the backhoe boom, the reference signal and the boom cylinder pressures and stroke is logged during several measurement operations. The measurement operations are performed for four different load cases, which are illustrated in Figure 5.2 and for eleven different reference signals, -100 to $100\,\%$ with intervals of $20\,\%$.

The reference signal is kept constant during each measurement, and the initial acceleration and final retardation of the cylinder are excluded in the measurements to only get the constant flow for each measurement. The flow into, or out from, chamber A is given by

$$q_{cA} = A_{cA}\frac{ds(t)}{dt}\ . \tag{5.3}$$

The resulting values for all measurements are used with MATLABs Curve Fitting Toolbox™ to get the surface representing the characteristics in Figure 5.3. As seen in the figure, at positive flow the flow decreases with an increased pressure for the same reference signal. This is not true for negative reference signals, where the flow increases for a higher pressure at the same reference signal. This implies that pressure feedback is not implemented at negative reference signals, i.e. at lowering of the boom.

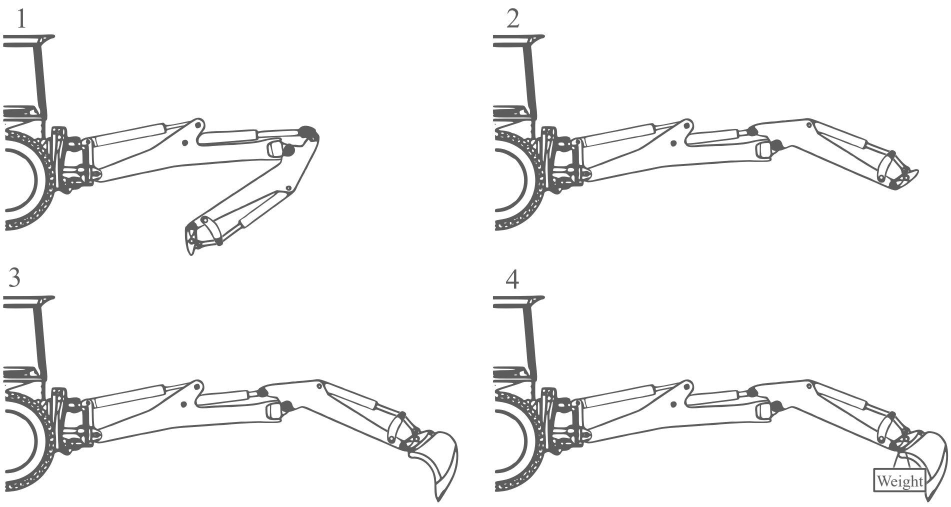

Figure 5.2: The different loads used during measurements for characteristics. 1. Folded backhoe, 2. Straight backhoe, 3. Straight backhoe with a bucket, 4. Straight backhoe with bucket and an extra weight.

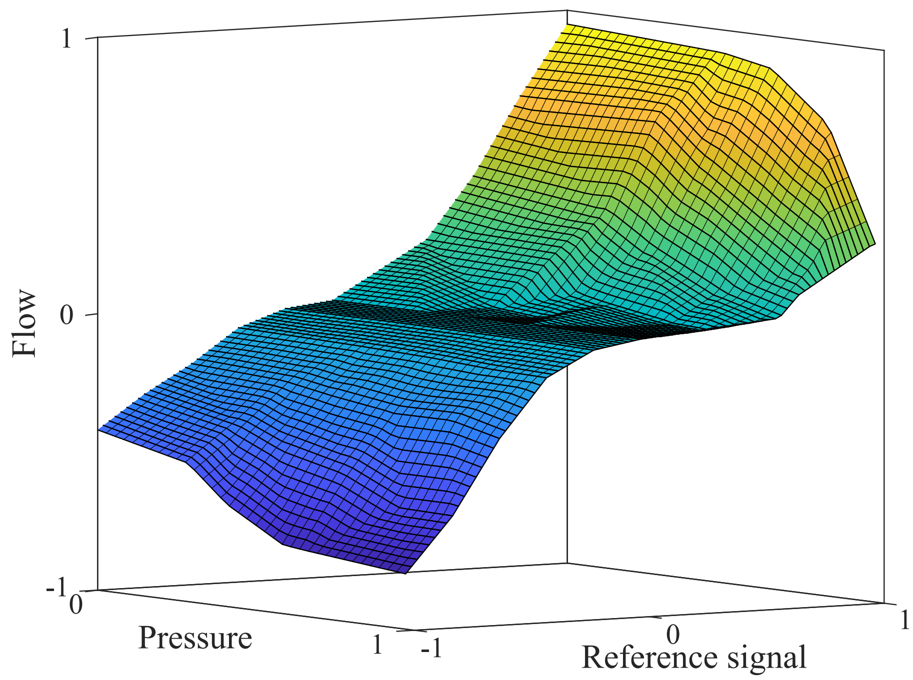

Figure 5.3: Backhoe boom cylinder characteristics. Note that all axis in the figure are normalised.

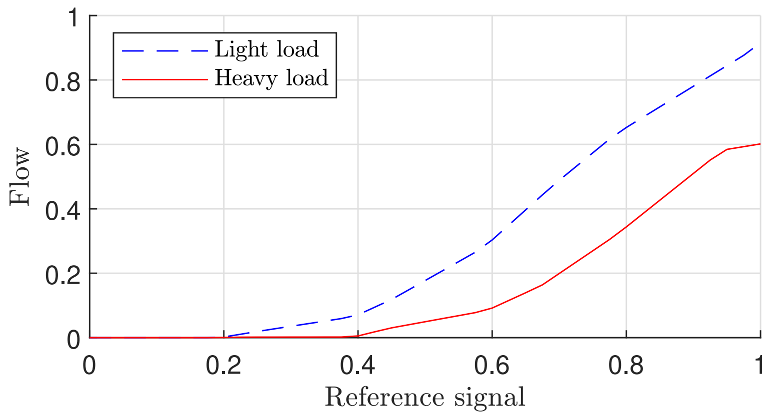

Figure 5.4: Characteristics for the boom cylinder for two different loads.

By comparing a 2D representation of the characteristics surface in Figure 5.3 for two different load cases, in Figure 5.4, the similarities with the illustration from Parker in Figure 5.1 is clear. The flow decreases with a higher load for the same reference signal. How the new system achieves similar characteristics is described in Section 6.2, and the resulting characteristics of the new system is presented in Section 5.3.

5.3 New System Characteristics

The resulting characteristics of the new system, with the implemented control strategy described in Section 6.2, is analysed for both a light and a heavy load case. During the light load case the pump pressure difference is up to approximately 100 bar and for the heavy load case up to 160 bar.

To validate the characteristics for dynamic operations, the requested flow from the characteristics map, in Figure 5.3, is compared to the measured flow with the original system, during the two load cases in Figures 5.5 and 5.6. During the heavy load case, in Figure 5.6, the requested flow follows the measured flow during lifting of the boom almost impeccably. During the light load case, the measured flow is up to 40 % lower than the requested flow. These results indicate that the characteristics map is more accurate for heavier loads than for lighter loads during lifting operation. During negative flow, the requested flow is slightly too low during heavy load and nearly perfect for light loads.

The same measurements were performed with the new, pump-controlled, system, with the results presented in Figures 5.7 and 5.8. The flow from the rig during these measurement for the new system follows the requested flow almost precisely during negative flow. The measured flow are marginally lower in the light load case during positive flow and up to 10 l/min to low during the heavy load case.

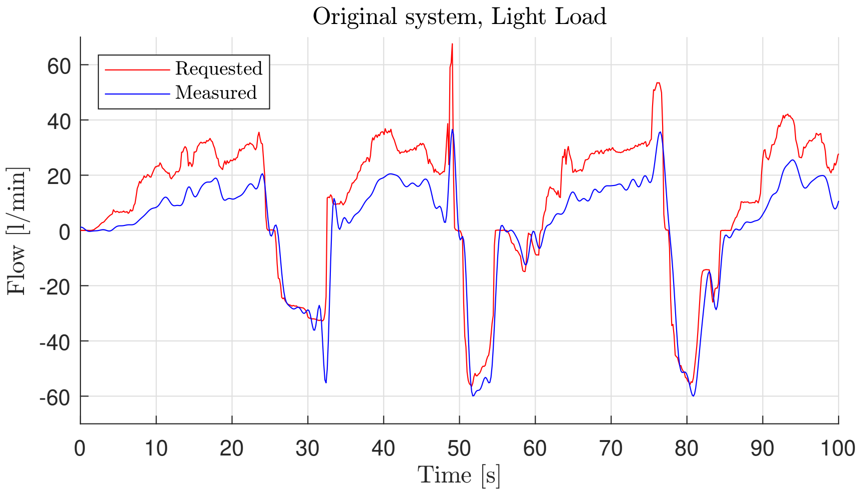

Figure 5.5: Flow comparison, during light load, between actual flow from the original system and the requested flow from the characteristics map.

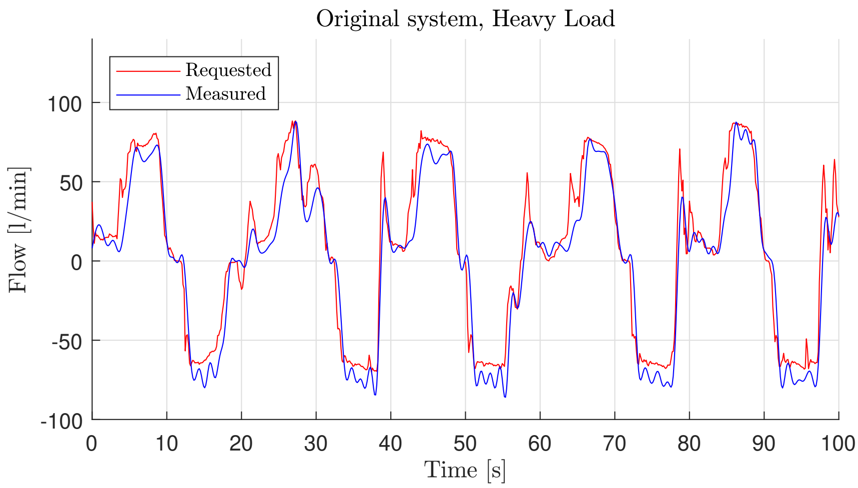

Figure 5.6: Flow comparison, during heavy load, between actual flow from the original system and the requested flow from the characteristics map.

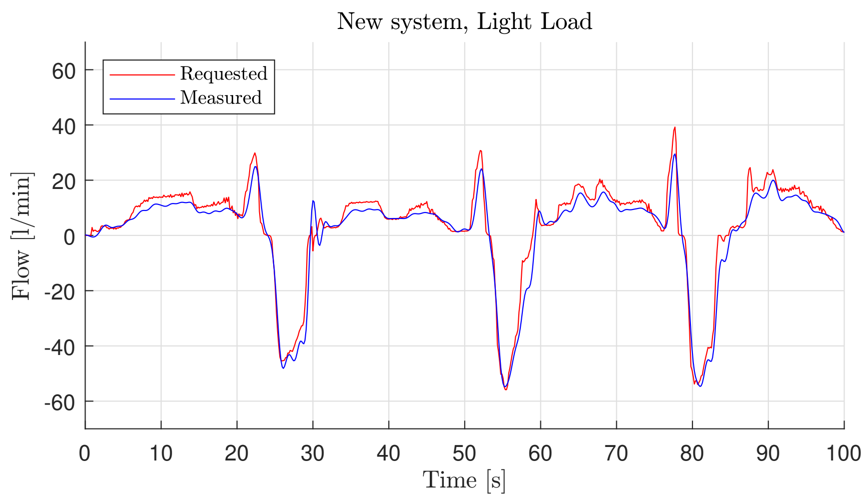

Figure 5.7: Flow comparison between requested flow and the actual flow from the the rig during the light load case.

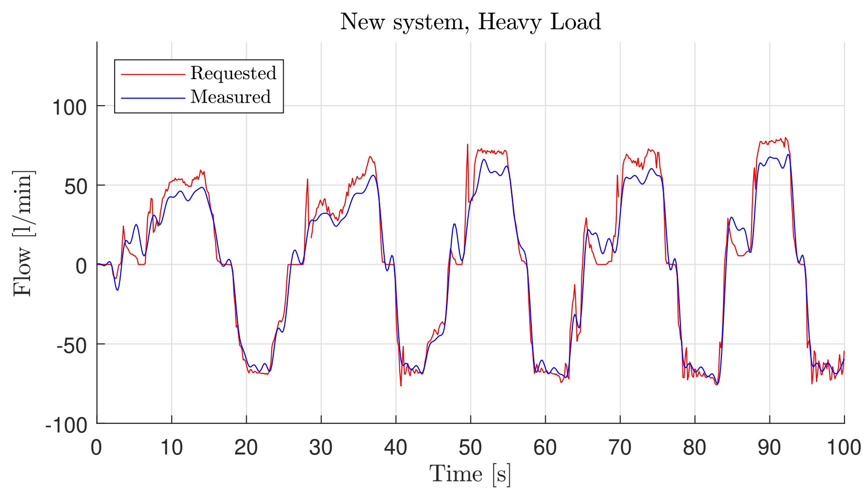

Figure 5.8: Flow comparison between requested flow and the actual flow from the the rig during the heavy load case.

Chapter 6

Control System

To minimise the energy consumption and to regenerate as much energy as possible the control system is of great importance. This chapter presents the used control system, how its been developed and implemented.

6.1 Control Strategy

A common approach in control system is to use a closed feedback loop, i.e. measure the output of the system and comparing it to a reference value. To use this approach, the output signal must be measurable. The output of the boom system is the speed of the cylinder or the flow into the cylinder. Huddig has, however, no plans today on implementing any position or flow transducers on the cylinders. It is therefore not desirable to use the stroke transducers in the control strategy. A closed feedback loop is consequently not possible to use. Instead of using a feedback signal from the cylinder to calculate the actual flow into the cylinder a model of the system is used to predict the flow depending on the rotational speed and displacement setting of the pump.

The general idea of the control system is illustrated in Figure 6.1. The characteristic presented in Chapter 5 is used in the first step to get the desired cylinder flow, q_{des}, depending on the reference signal, r, from the operator and the current pressure in chamber A and B, p_{cA} and p_{cB}, of the boom cylinder. The control strategy then uses the desired flow from the characteristics map, the pump pressures, p_{pA} and p_{pB}, and the volumetric efficiency map of the pump to choose an rotational speed and displacement setting.

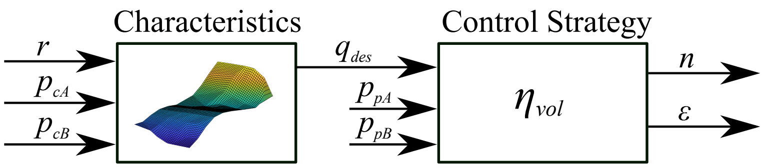

Figure 6.1: General control system strategy.

In some operations the pump flow is not the same as the cylinder flow in chamber A, as seen for quadrant 3 in Figure 3.8. The added area compensation flow, $q_{\Delta A}$, from the boost pump is included in the pump flow for operations in quadrant 3. The desired pump flow, q_p, is thus given by

$$q_p = \begin{cases} q_{des} + q_{\Delta A}, & \text{if } p_{pA} < p_{pB} \text{ and } q_{des} > 0 \\ q_{des}, & \text{else} \end{cases} . \tag{6.1}$$

The volumetric efficiency, $\eta_{vol,p}$, of the pump is used to predict the flow from the pump depending on the rotational speed, displacement setting and pump pressure. During operations in quadrant 1 and 3, when the hydraulic machine is in pump mode, the predicted flow is calculated by

$$q_p = \begin{cases} nD\varepsilon\eta_{vol,p} + q_{\Delta A}, & \text{if } p_{pA} > p_{pB} \text{ and } q_{des} > 0 \\ nD\varepsilon\eta_{vol,p}, & \text{else} \end{cases} . \tag{6.2}$$

If the pump is instead in motor mode, in quadrant 2 or 4, the flow is calculated by

$$q_m = nD\varepsilon\frac{1}{\eta_{vol,p}} . \tag{6.3}$$

The displacement, D, is a known parameter of the pump, the rotational speed, n, and displacement setting, ε, are variables in the control strategy. The volumetric efficiency, $\eta_{vol,p}$, is given by an efficiency map provided by the manufacturer of the pump. The map however lacked data for low displacement settings. By measuring the speed of the cylinder at different displacement settings, different rotational speeds and at different loads the efficiency map was supplemented.

With the desired pump flow from Equation (6.1) and the prediction model in in Equations (6.2) and (6.3), the two control variables, n and ε, can be determined.

6.2 Implemented Control Strategy

The control strategy evaluated in [8] and described in Section 2.3 requires many parameters describing the dynamic behaviour of the used components. For example the acceleration of the electric motor, displacement setting speed and moment of inertia for both pump and electric motor. Since these parameters are unknown for the used components, this control strategy cannot be implemented in the new system. A different control strategy, that for any desired flow and pressure difference over the pump, can choose an optimal speed and displacement setting that minimises the energy consumption was evaluated during the project. This control strategy requires complete efficiency maps for the mechanic efficiency for the EMG, and both the hydro mechanic and volumetric efficiencies for the pump. But, due to lack of data in the maps and no available tools to measure the mechanic efficiency, this control strategy could not be implemented. However, the available data indicated that the largest portion of the total loss originates from the volumetric losses due to the low maximum displacement setting.

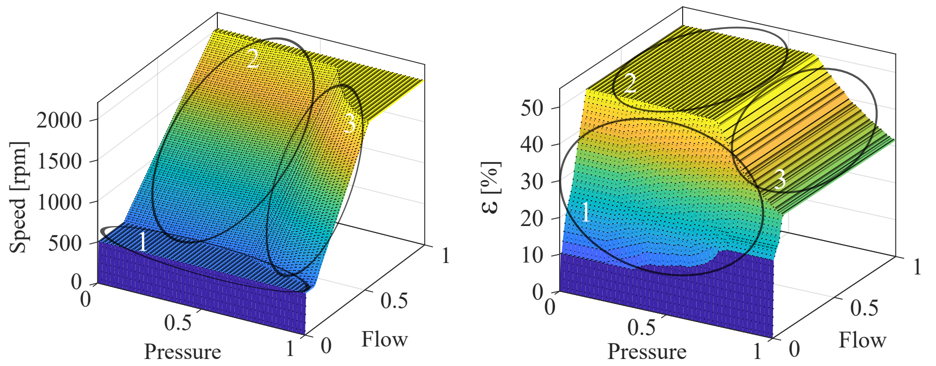

(a) Map for the rotational speed. (b) Map for the displacement setting.

Figure 6.2: Precalculated maps for speed and displacement setting for pump operation, as function of desired flow and current pressure difference over the pump.

The implemented control strategy is based on a simpler approach. On direct input from the operator lever, the EMG is initiated and the rotational speed is set to the pumps minimum allowed speed, 500 rpm. When the characteristic map requests a flow, two precalculated maps are used to decide the rotational speed and displacement setting of the pump. These maps are illustrated in Figure 6.2. To maximise the efficiency, the displacement setting is set as high as possible, but due to the minimal rotational speed for the pump, the system is displacement controlled for flows below approximately 25 l/min. For a pressure difference above 155 bar over the pump, the required torque is higher than the available torque from the EMG. The maximum available torque on the EMG is, according to Table 4.1, 185 Nm, but due to the internal boost pump and hydro mechanic losses in the pump the available torque for the main pump is estimated to be 155 Nm.

As seen in Figure 6.2 the maps are divided into three operation areas where the speed and displacement are calculated differently from each other. The flow is in the first area controlled by the displacement with a constant rotational speed. In the second area the displacement setting is constant at 50 % and the flow is controlled by the rotational speed. The third area is where the available torque is insufficient to have the maximum displacement setting on the pump so the displacement setting is therefore calculated by the available torque and the pressure difference over the pump. All according to Equations (6.4) and (6.5)

$$\varepsilon = \begin{cases} \dfrac{q}{nD\eta_{vol,p}}, & \text{if Area 1} \\ \varepsilon_{max}, & \text{if Area 2} \\ \dfrac{2\pi\, T_{max}}{D\Delta p} & \text{if Area 3} \end{cases} \tag{6.4}$$

$$n = \begin{cases} n_{min}, & \text{if Area 1} \\ \dfrac{q}{\varepsilon D\eta_{vol,p}}, & \text{if Area 2 or 3} \end{cases} \tag{6.5}$$

Chapter 7

Energy Analysis

The new system is compared to the original in three different tests. How these tests have been conducted, the results obtained and an analysis of the results are presented in this chapter.

7.1 Equations

The equations used for analysing the energy and power usage for the original and new hydraulic systems are presented in this section.

7.1.1 Energy and Power Calculations

To be able to analyse the different components of the new system, the power is measured in different parts of the system to investigate the energy recovery and energy efficiency. The potential power is calculated by first finding the CoG of the backhoe and any attached tools or weights using the cylinder strokes and the weights of all major parts of the backhoe. The potential power can then be calculated using the gravitational force and vertical velocity:

$$P_{pot} = F_{mg} v_{v,CoG} = mg \; v_{v,CoG} = mg \; \frac{dh_{CoG}}{dt} \; . \tag{7.1}$$

A more detailed description of how the potential power is calculated and how the position of the CoG is found is described in Appendix A.

The hydraulic power in the cylinder is calculated, using the cylinder pressures and the flow, using the following equation:

$$P_{cyl} = F_{load} v_{cyl} = (p_{cA} A_A - p_{cB} A_B) \frac{ds}{dt} \; . \tag{7.2}$$

Since there is no leakage in the A side of the system, the flow into the pump can be calculated using the speed of the cylinder and the area of cylinder chamber A. If the pressure in the B side of the system is higher than on the A side, the area compensation flow, $q_{\Delta A}$, is added to the flow into the pump. The hydraulic power in the pump is thus defined by

$$P_p = \begin{cases} \Delta p_p \ q_{cA}, & \text{if } p_{pA} \geq p_{pB} \\ \Delta p_p \ (q_{cA} + q_{\Delta A}), & \text{if } p_{pA} < p_{pB} \end{cases} . \tag{7.3}$$

The power from, or charged into, the battery is simply defined as:

$$P_{bat} = UI \ . \tag{7.4}$$

With the power calculated in Equations (7.1) to (7.4), each parts accumulated energy can be calculated by

$$E = \int P(t)dt \ . \tag{7.5}$$

7.1.2 Efficiency Calculations

The efficiency is, as known, calculated from the used energy and the obtained useful energy,

$$\eta = \frac{E_{useful}}{E_{used}} \ . \tag{7.6}$$

For the complete boom cylinder system the used and useful energy is different depending on if the system is lifting or lowering the boom. The used energy when lifting the boom is the energy from the battery and the gained useful energy is the increase of potential energy of the backhoe. During lowering the used energy is the potential energy and the useful energy is the energy charged into the battery. The efficiencies are thus defined as

$$\eta_{lifting} = \frac{E_{pot}}{E_{bat}} \tag{7.7}$$

and

$$\eta_{lowering} = \frac{E_{bat}}{E_{pot}} \ . \tag{7.8}$$

The efficiency of individual parts of the system is calculated in a similar way using the equations in Section 7.1.1 and the energy flow charts in Figures 7.1 and 7.2.

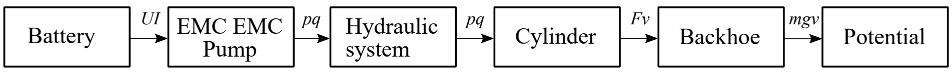

Figure 7.1: Positive energy flow during lifting of the backhoe and with which physical quantities the power is calculated.

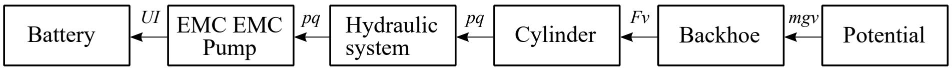

Figure 7.2: Positive energy flow during lowering of the backhoe and with which physical quantities the power is calculated.

7.2 Energy Recovery

The purpose of this test is to investigate the energy recovery performance for the backhoe. The energy consumption and efficiency when lifting and lowering the backhoe in a predefined motion and load. Thus the energy used to lift the CoG of the backhoe a certain height at a certain speed. During the lifting operation, the energy input is the energy from the battery and the useful energy output is the increased potential energy. During the lowering operation, the input is the potential energy and the output is the energy charged into the battery. During the measurements of the test, the boom cylinder is kept at a constant speed to avoid acceleration of the backhoe. However, since the CoG of the backhoe moves in a circular motion all acceleration of the backhoe can not be avoided. The acceleration of the CoG of the backhoe is so small that it is assumed to be negligible. All measurements in the test are carried out in the same way which makes them comparable to each other.

The test is performed to replicate the backhoe positioned in Figure 7.3 with the bucket half loaded with gravel. To get more accurate results, longer measurements are desired. To be able to run the test for a longer cylinder stroke without the bucket hitting the floor the positioning of the dipper is changed by retracting the dipper cylinder as illustrated in Figure 7.4. To compensate for the changed position of the dipper the mass of the gravel in the bucket is lowered to get the same resulting pressure in the boom cylinder. During this test the pressure difference

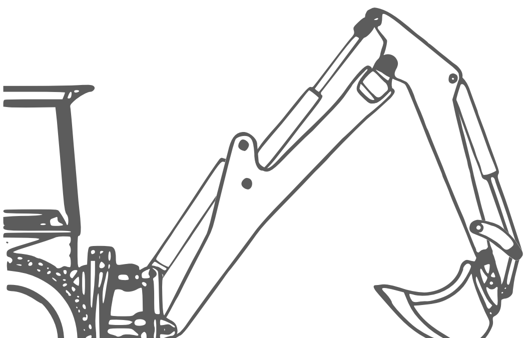

Figure 7.3: Illustration of the positioning of the backhoe that the energy recovery test is performed to replicate.

over the cylinder is approximately 130 bar. The test is performed for seven different flows into or out from cylinder chamber A, 10, 20, 30, 40, 50, 60 and 70 l/min, in both lifting and lowering operation.

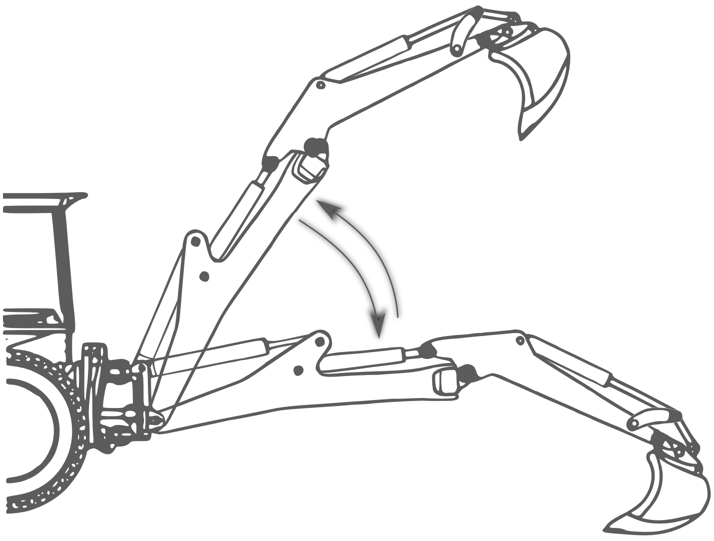

Figure 7.4: Illustration of energy recovery test.

The efficiency at different flows for lifting of the backhoe is presented in Figure 7.5a. When using the new system compared to the original, the efficiency is increased by 8 to 20 % at flows from 10 to 70 l/min. The flows where the efficiency is most increased are between 20 and 40 l/min. During lowering operation the original system still uses energy from the battery to power the hydraulic pump to produce flow into cylinder chamber B. The efficiency for the original system is therefore negative as can be seen in Figure 7.5b. In the new system, for flows of 17 l/min or above the potential energy is powering the pump through the flow and pressure in the hydraulic system. The hydraulic pump now acts as a motor and the EMG acts as a generator that charges the battery. During this measurement with a cylinder pressure difference of 130 bar, flows of less than 17 l/min is insufficient to power the hydraulic pump, resulting in the EMG has to assist. The EMG therefore uses battery energy resulting in a negative efficiency which also can be seen in Figure 7.5b.

The new system has a regeneration efficiency during a lifting and lowering cycle at the same flow up and down of up to 18 %, represented by the green line in Figure 7.6. The highest efficiency during lifting is at 60 l/min and is 48 %, for lowering the optimal flow is 40 l/min and has an efficiency of 39 %.

As can be seen in Figure 7.6, the lifting efficiency is between 29 and 48 % for all measured flows. The lowering efficiency however varies from a negative efficiency below 17 l/min up to 39 % at 40 l/min and then goes down towards 20 % at 70 l/min. The lowering efficiency thus depends more on the flow than the lifting efficiency. To understand why, the total efficiency is split up into multiple

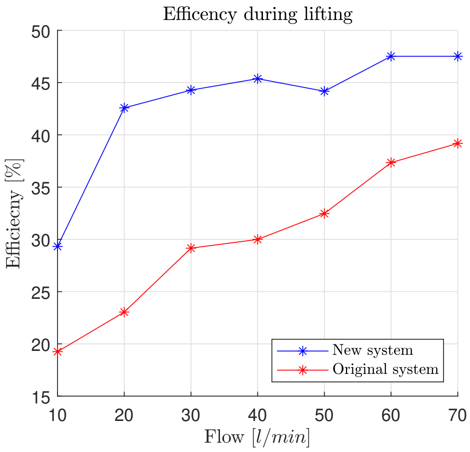

(a) Energy efficiency during lifting operation at different cylinder flows.

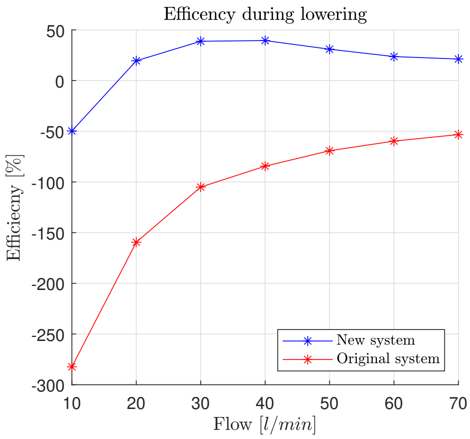

(b) Energy efficiency during lowering operation at different cylinder flows.

Figure 7.5: Energy efficiency for the regeneration test for a cylinder pressure difference of 130 bar. Note the different scales on the efficiency axis in the two figures.

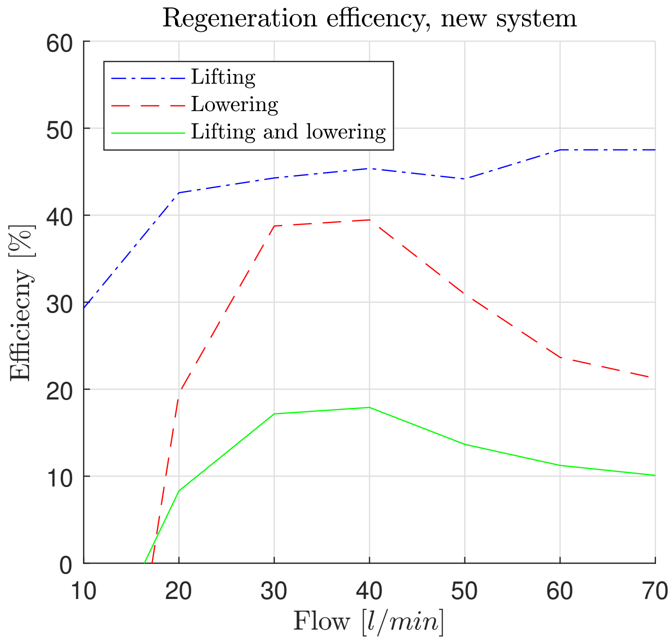

Figure 7.6: Energy efficiency for the new system during lifting, lowering and both lifting and lowering.

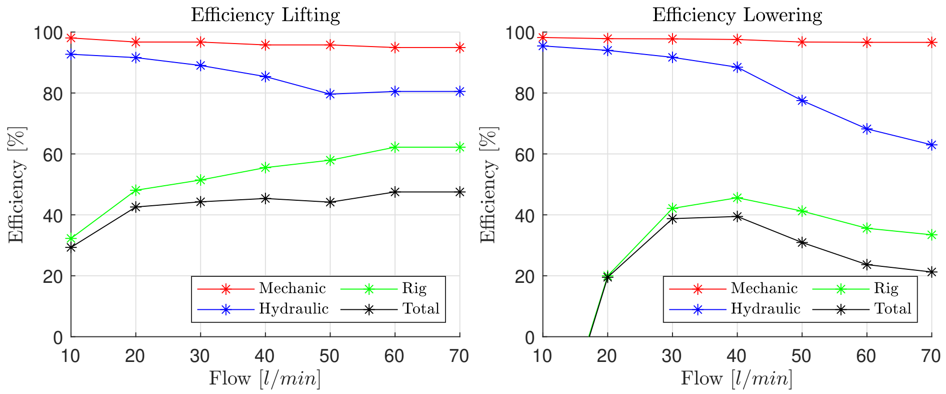

(a) The new systems parts different efficiencies during lifting.

(b) The new systems parts different efficiencies during lowering.

Figure 7.7: The total efficiency split up over three different parts of the system. The mechanic efficiency includes the backhoe and boom cylinder. The hydraulic part includes the hoses and the LHV. The rig including the EMC, EMG and pump.

efficiencies for different parts of the system, presented in Figure 7.7. During lowering operation the mechanic efficiency, including friction losses in the backhoe and boom cylinder, keeps almost constant for all flows, as seen in Figure 7.7b. The hydraulic efficiency, including the hoses and LHV, reduces with increased flow. This is explained by the higher pressure drop over the LHV at higher flows, described in Section 4.2.3 and in Figure 4.9. The increase of the total efficiency from 10 to 30 l/min is due to the increase of efficiency of the components in the rig, the pump, EMG and EMC.

Figure 7.8 clarifies and compares the energy used in the lifting and lowering cycle for the two systems. The energy used from, or charged into, the battery is normalised against the potential energy gained and lost during the cycle. It can be noted that the new system uses less energy during the lifting operation than the original system and regenerates the battery during the lowering operation. The original system, however, still uses energy during the lowering operation which also was described above and can be seen by the negative efficiency in Figure 7.5b. It can be seen in all graphs in Figure 7.8 that the energy used after the whole cycle for the new system is approximately half of what the original system uses.

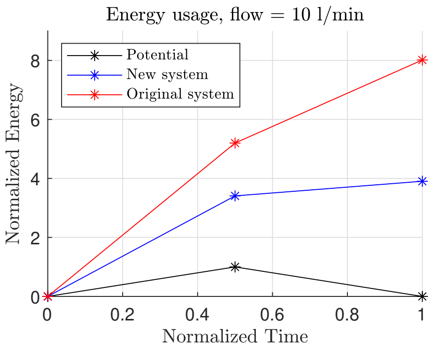

(a) Energy usage at 10 l/min.

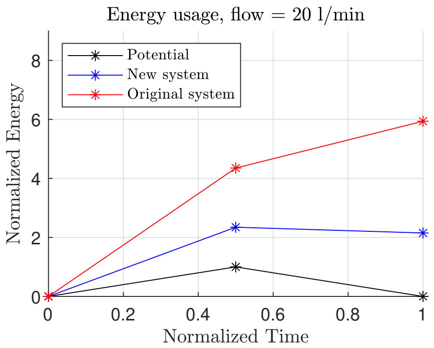

(b) Energy usage at 20 l/min.

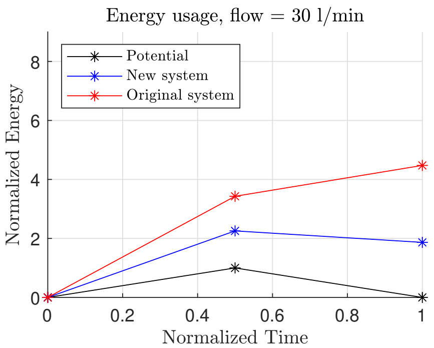

(c) Energy usage at 30 l/min.

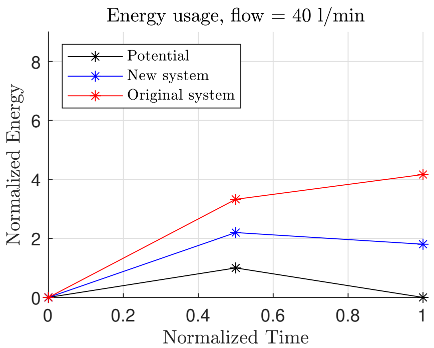

(d) Energy usage at 40 l/min.

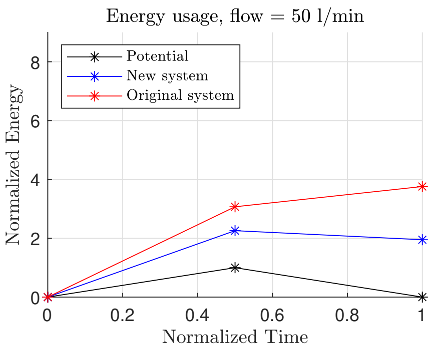

(e) Energy usage at 50 l/min.

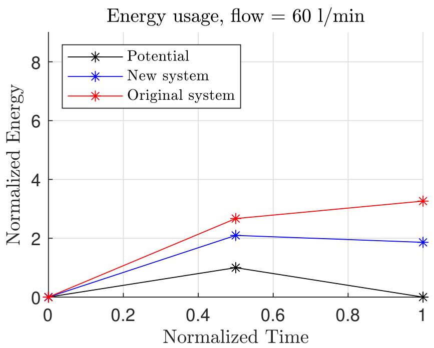

(f) Energy usage at 60 l/min.

Figure 7.8: Normalised energy consumption for a lifting and lowering cycle with flows between 10 and 60 l/min. The energy used and regenerated is normalised against the gained or lost potential energy.

7.3 Excavating

One of the most energy consuming operations for the backhoe is, according to Huddig, excavating. Excavating sand, soil or gravel out of a pit and unloading it onto a high pile or a hauler. The motion of this operation is illustrated in Figure 7.9 and is used to compare a high duty and high energy consuming cycle for the two systems. During actual excavating the boom slew is used to relocate the mass sideways, this is not performed during this test. The bucket is filled with sand in each cycle and unloaded straight back into the pit so the cycle is more easily repeated.

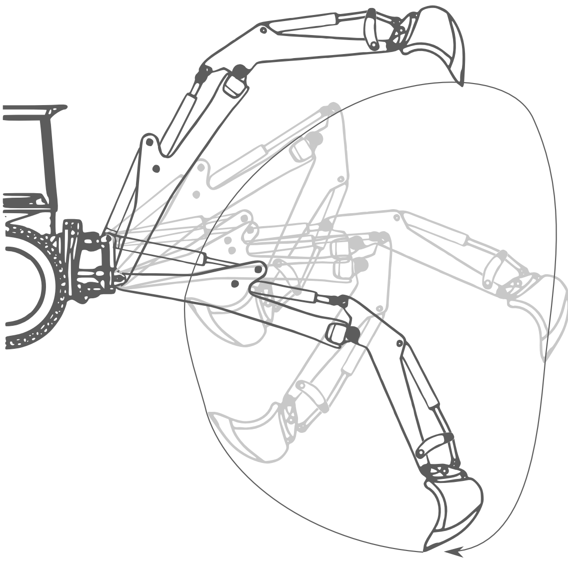

Figure 7.9: Cycle for the excavating test.

7.3.1 Backhoe Movement

During the measurements the excavating and unloading cycle is repeated seven times for each system. The exact motion of the backhoe is however hard to replicate in the repeated cycles. To investigate if the two measurements for the two systems are comparable to each other, the lifting height and lifted mass are compared. The vertical position of the bucket, in Figure 7.10, represents how high the load has been lifted. As seen in the figure, the vertical position of the bucket is approximately the same over the seven cycles but with a varied time offset, indicating that the lifted height is comparable between the measurements.

The time duration for the excavation test for the original and new system were 145 s and 136 s respectively. The measurements differed by 8 s, so in order to more easily compare the load during the two measurements, the time has been normalised in Figures 7.11 to 7.13. Figure 7.11 illustrates the horizontal length

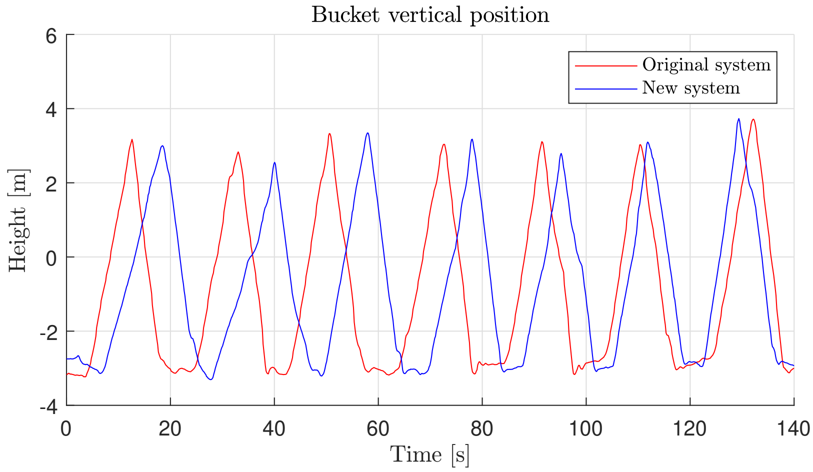

Figure 7.10: Bucket position comparison between the two excavating measurements.

between the boom hinge and the bucket, i.e. the length of the lever of the mass in the bucket. As seen in the figure, the lever length is shorter during lifting of the bucket for the original system. This would, for the same mass in the bucket, result in a lower boom cylinder pressure. For excavating cycle 2 (Time 0.20-0.25) and 7 (Time 0.88-0.91) the difference in lever length is most evident. The difference of the cylinder pressure for these two cycles are also distinctly lower for the original system seen in Figure 7.12. To compare the lifted load for the two measurements

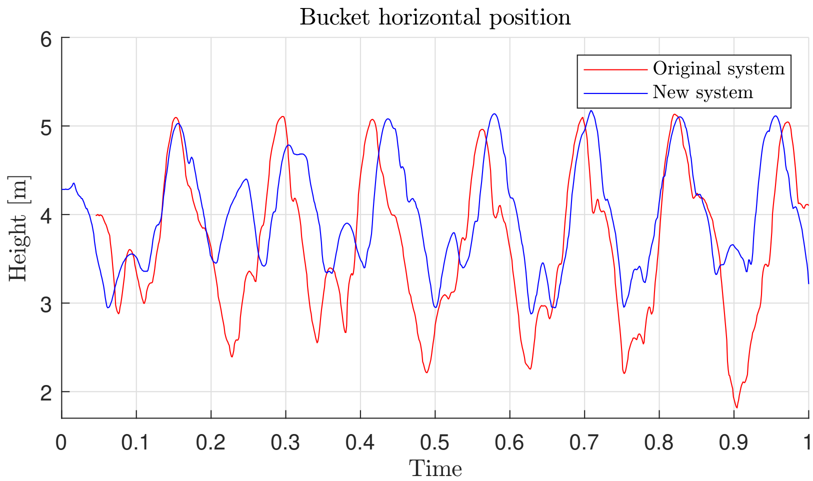

Figure 7.11: Comparison of the horizontal position of the bucket between the two excavating measurements.

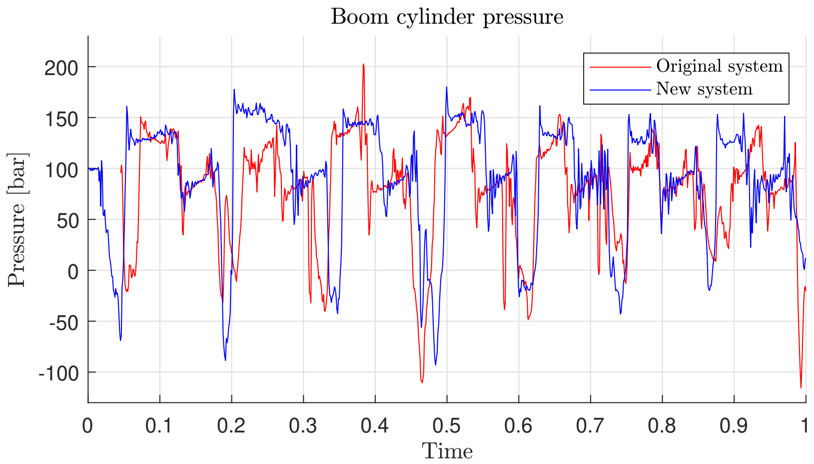

Figure 7.12: Pressure difference over the boom cylinder.

Equation (7.9) is used to calculate the ratio, φ, between the cylinder pressure, Δp_{cyl}, and the bucket lever length, l_{lever}.

$$\varphi = \frac{\Delta p_{cyl}}{l_{lever}} \tag{7.9}$$

The result for this comparison is presented in Figure 7.13, and it can be seen that the load mostly follows the same pattern for the two measurements. This indicates that the amount of mass lifted is approximately the same during the two measurements. The measurements are thus considered to be sufficiently equal to be able to compare the energy and power consumption for the two systems.

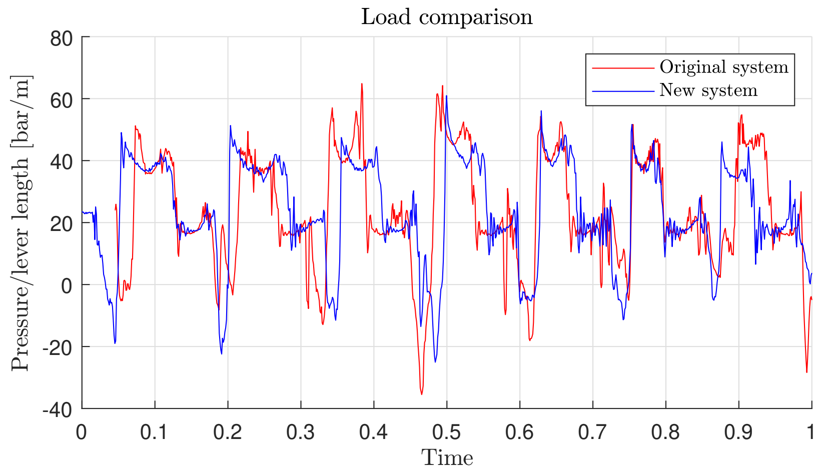

Figure 7.13: Load comparison for the two measurements.

7.3.2 Energy Comparison

Since the sectioning of the new hydraulic system removes the boom cylinder from the original system, the pump on the Tigon machine only needs to supply the maximum required pressure from the dipper and bucket cylinder. If the boom cylinder has the highest pressure during the excavation the system pressure on the Tigon machine would be decreased for the new system compared to the original. This is illustrated by Figure 7.14 where it is clear that the Tigon pump pressure is decreased for all cycles during the measurement for the new system compared to the original.

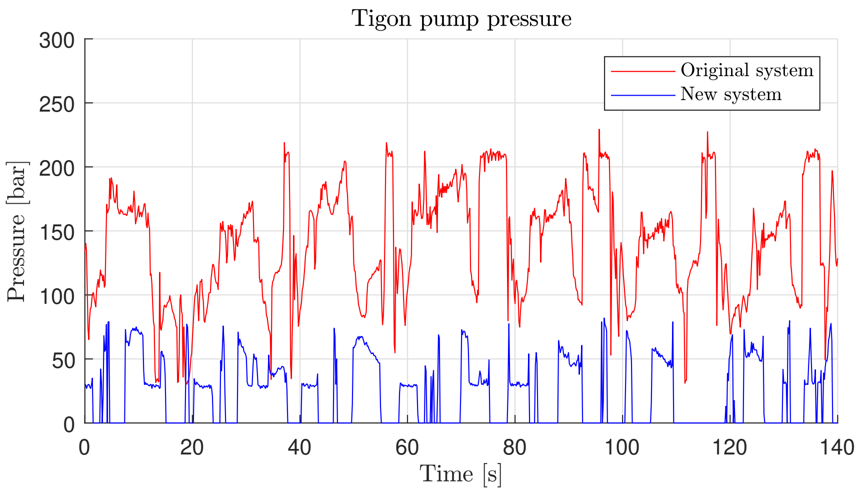

Figure 7.14: System pressure on the Tigon machine for the original and new system during the excavation test.

The average pump pressure, excluding pressures at 0 bar, during the entire measurement is 140 bar for the original system and 45 bar for the new system. By sectioning the hydraulic circuit into two separate systems the required hydraulic power to the dipper and bucket cylinder has decreased by 68 %, assuming the same flow for the two systems. The reduced energy requirement is explained by the reduced throttling losses due to the differences in load pressure, illustrated by Figures 3.5 and 3.9.

This can also be seen by investigating the total used hydraulic energy for the two systems. The used hydraulic power for the original system is:

$$P_{hydraulic,original} = p_p \left(q_{cyl1} + q_{cyl2} + q_{cyl3}\right), \tag{7.10}$$

and

$$P_{hydraulic,new} = p_{p,rigg} q_{cyl1} + p_{Boost} q_{\Delta A} + p_{p,Tigon} \left(q_{cyl2} + q_{cyl3}\right) \tag{7.11}$$

for the new system. By integrating these powers over the total measurements, the energy usage for the two systems is obtained and presented in Figure 7.15. As

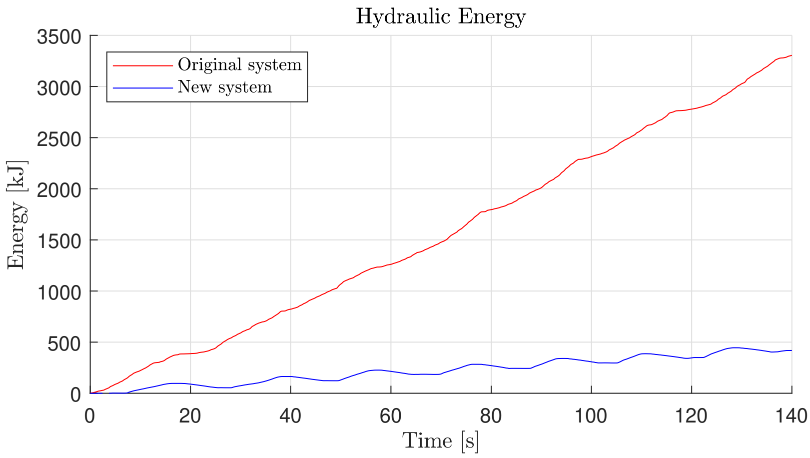

Figure 7.15: Used hydraulic power for the different systems.

seen in the figure, the hydraulic energy for the new system is significantly lower than for the original system. The resulting used hydraulic energy for the seven excavating cycles for the original system is 3300 kJ and only 420 kJ for the new system. A vast hydraulic energy reduction of 87 %. As Figure 7.14 illustrates, the pump pressure on the Tigon, and so fourth the power to the dipper and bucket cylinder, is reduced by 68 %. The boom cylinder power is also reduced, both by minimising throttling losses by removing the flow direction valve, but mostly due to the capability of recovering the energy when lowering the boom, which is illustrated by the dashed line in Figure 7.16. The used hydraulic energy for the boom cylinder is 622 kJ, and regained is 309 kJ, resulting in the used net hydraulic energy of 313 kJ. The regained hydraulic energy is thus almost half of the used hydraulic energy.

The used electric energy combined with the used hydraulic energy for both systems are presented in Figure 7.17. As seen in the figure, the used electric energy for the original system is just over 1000 kJ over the hydraulic energy. This implies that with an EMC, EMG and pump with an efficiency of 100 % the used electric energy for the original system will still be slightly higher than the actually used electric energy for the new system. The new system, with a decoupled circuit for the boom cylinder and components not suitable for this kind of system, has great potential for improvement and yet has a energy savings of over 30 % during excavating.

The hydraulic and electric power during the measurement for rig on the new system is presented in Figure 7.18. During lifting, i.e. positive power, the efficiency of the EMC, EMG and pump is up to between 50 and 70 % and during lowering an efficiency of up to 40 %. These values correlates well with the analysis of for the energy recovery test presented in Figure 7.7. During the recovery test the rig had an efficiency during lifting between 50 and 63 % for flows above 30 l/min. During lowering of the boom the rig had an negative efficiency for flow below 17 l/min

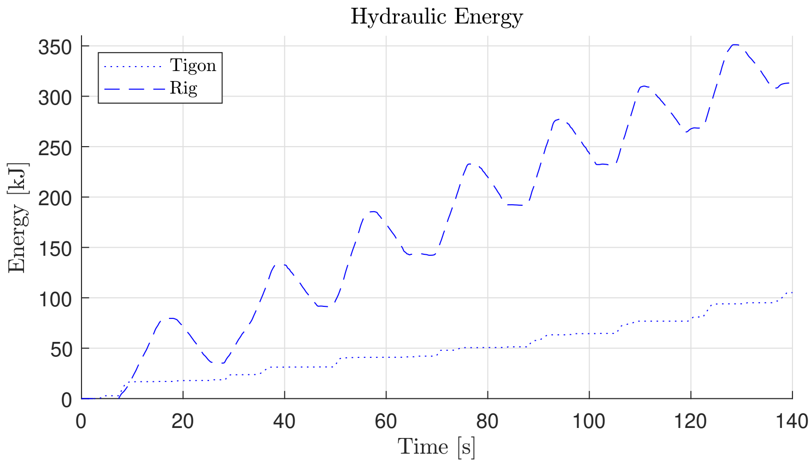

Figure 7.16: Net hydraulic energy used by the Tigon and the rig during the measurement for the new system.

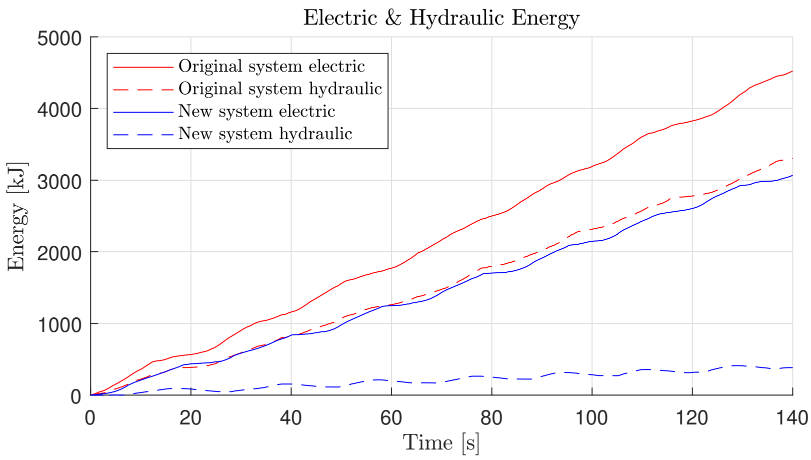

Figure 7.17: Used hydraulic and electric power for the different systems.

and up to 45 % at 40 l/min.

The amount of regenerated energy during excavation is illustrated in Figure 7.19 together with the cumulative used and regenerated energy. The proportion of regenerated energy stabilises towards 8 %. Even though work is performed during the test by lifting sand 8 % of the energy consumed is regenerated back into the battery.

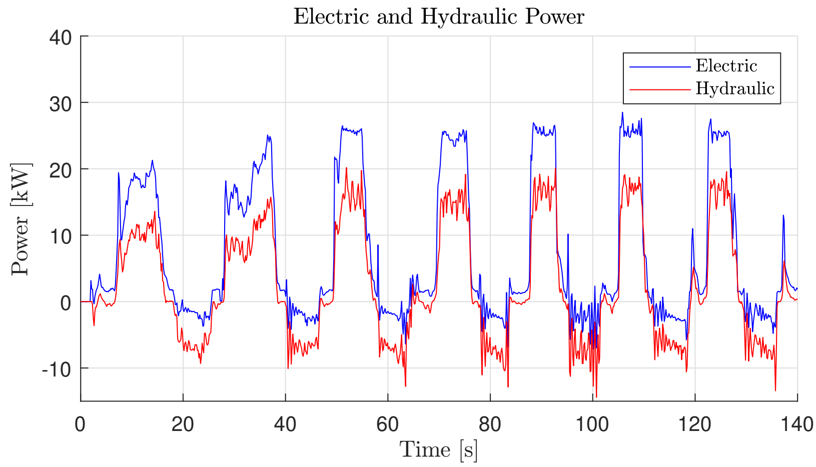

Figure 7.18: Used and regenerated power by the rig.

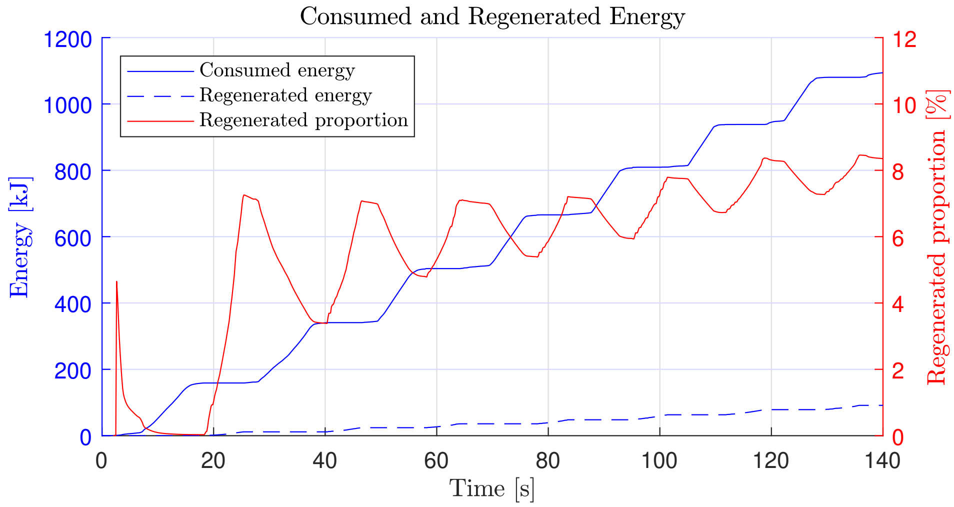

Figure 7.19: Used and regenerated energy for the rig during the excavation test. The proportion of regenerated energy compared to used energy.

7.4 Grading

To compare the two systems at a lower energy consuming operation, two measurements are performed where the backhoe is used for grading. The purpose of grading is to level out the ground surface. This is accomplished by keeping the bucket at the same height while lifting the boom and retracting the dipper at a slow pace, illustrated in Figure 7.20. The test is performed indoors and there is no mass in the bucket during any part of the test.

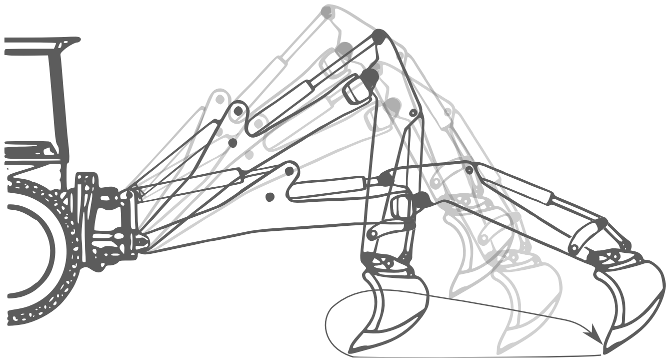

Figure 7.20: Illustration of the backhoes position during the grading test.

7.4.1 Backhoe Movement

During the measurements, the grading movement is repeated six times for both the original system and the new system with the implemented rig for the boom cylinder. As mentioned for the excavation test, the exact motion is near impossible to repeat, to investigate if the two measurements are comparable the boom and dipper cylinders stroke positions are compared and presented in Figures 7.21 and 7.22. The stroke position of the boom and dipper cylinder follows the same pattern but the boom cylinder is extended longer and the cylinder for the dipper is retracted more during the measurement for the original system. To check if the load is the same for the two measurements, the pressure difference across the boom cylinder is compared and presented in Figure 7.23. The two measurements are coherent to each other except some minor peaks, so the load is considered to be equal. The results for comparing the measurement indicates that the origi-

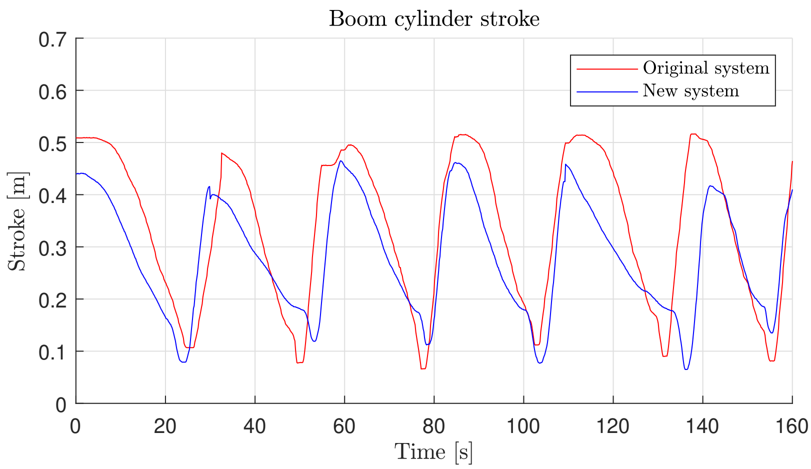

Figure 7.21: Boom cylinder stroke position during the grading measurements.

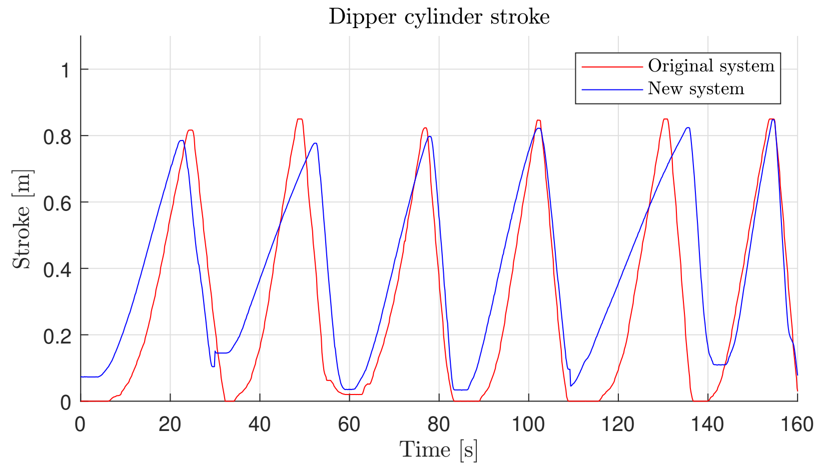

Figure 7.22: Dipper cylinder stroke position during the grading measurements.

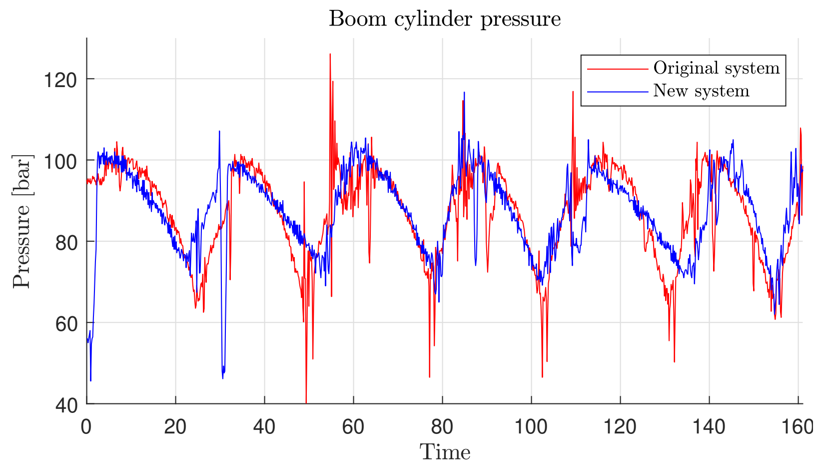

Figure 7.23: Pressure difference over the boom cylinder for the two measurements.

nal system has a slightly more energy demanding measurement. The difference is however considered to be small enough for the measurements to be sufficiently equal and comparable to each other.

7.4.2 Energy Comparison

The total cumulative net hydraulic and electric energy consumed during the two measurements are presented in Figure 7.24. During the six grading cycles the original system used 1700 kJ of hydraulic energy from the pump while the new systems hydraulic energy net use were only 120 kJ. Approximately half of this energy saving comes from the sectioning of the system. The pump pressure on

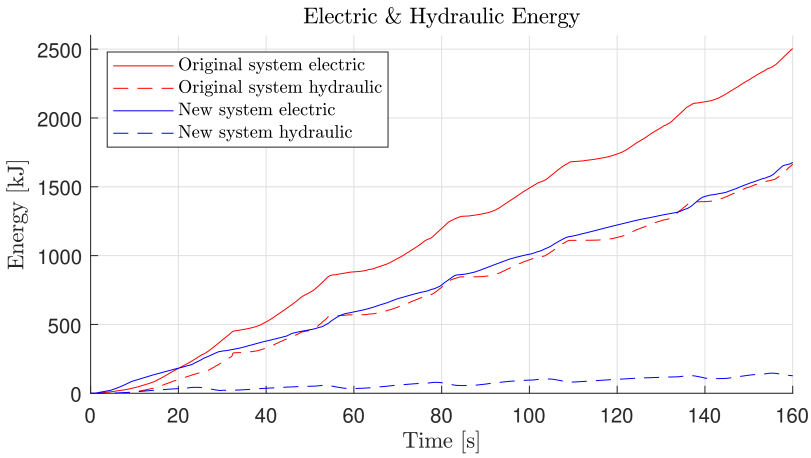

Figure 7.24: Accumulated electric and hydraulic energy consumption during the grading test.

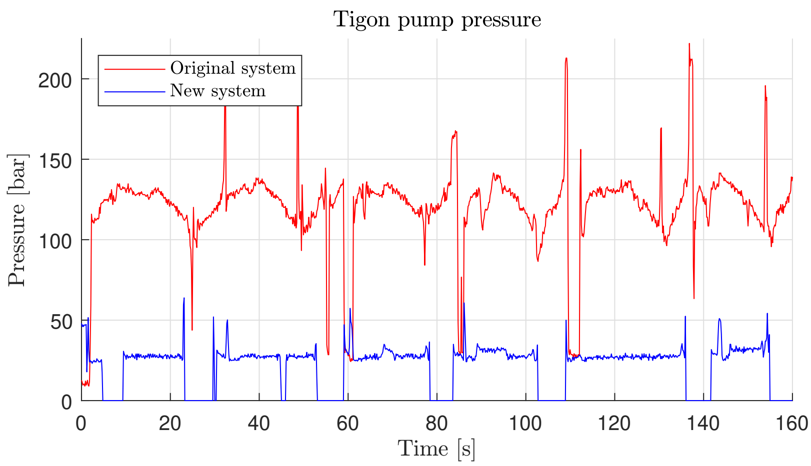

Figure 7.25: Tigon pump pressure.

the Tigon is reduced from 120 to 30 bar as illustrated in Figure 7.25 when using the new system compared to the original. With a accumulated flow of 80 l into the cylinder for the dipper and a pressure difference of 90 bar the saved hydraulic energy used by the dipper in the new system is approximately 700 kJ. The second half is due to the hydraulic regeneration on the rig illustrated by the dashed line in Figure 7.26. During extension of the boom cylinder the rig regains energy from the decreased potential energy resulting in a reduced net energy use. The original system still has to supply the flow into the B chamber of the cylinder during extension, which leads to increased hydraulic energy output.

The electric energy used by the new system is not as reduced as the hydraulic

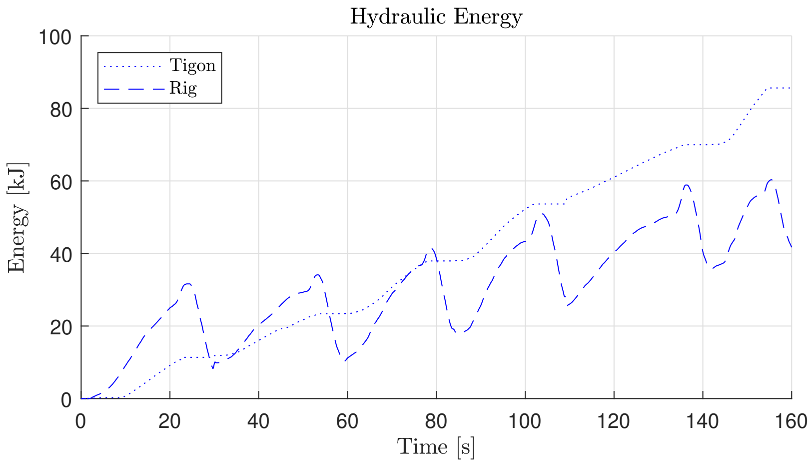

Figure 7.26: Net hydraulic energy used by the Tigon and the rig during the measurement for the new system.

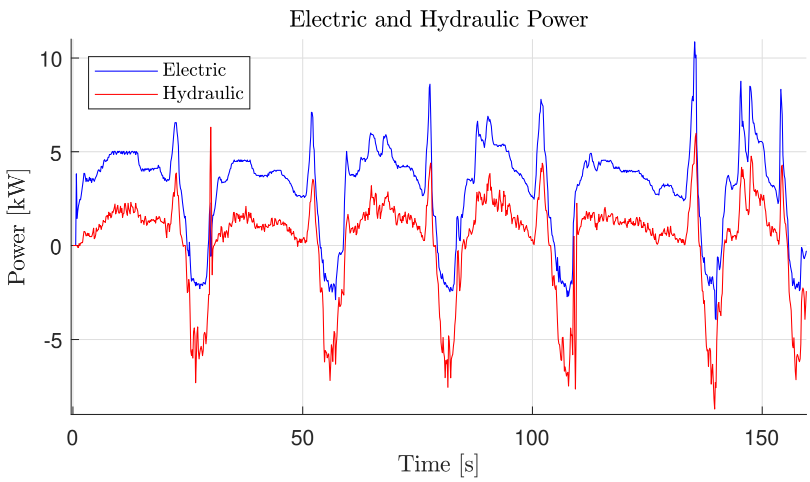

Figure 7.27: Electric and hydraulic power used, during the grading test.

energy due to the relatively low efficiency of the hydraulic pump for these operating points. The electric energy is reduced from 2500 kJ to 1700 kJ. The new system uses 30 % less energy compared to the original system, which is the same energy saving as for the excavating test.

The efficiency of the rig during the grading test is investigated by comparing the used hydraulic and electric power. The result is presented in 7.27 and indicates a maximum efficiency during boom lifting of 47 %. During lowering of the boom, the efficiency is up to 40 %. These values correlates with the efficiency of the rig during the energy recovery and the excavating test.

The cumulative used and regenerated electric energy illustrated in Figure 7.24

are presented together with the quotient between the two in Figure 7.28. The regenerated energy during the entire test is almost 8 % of the used energy.

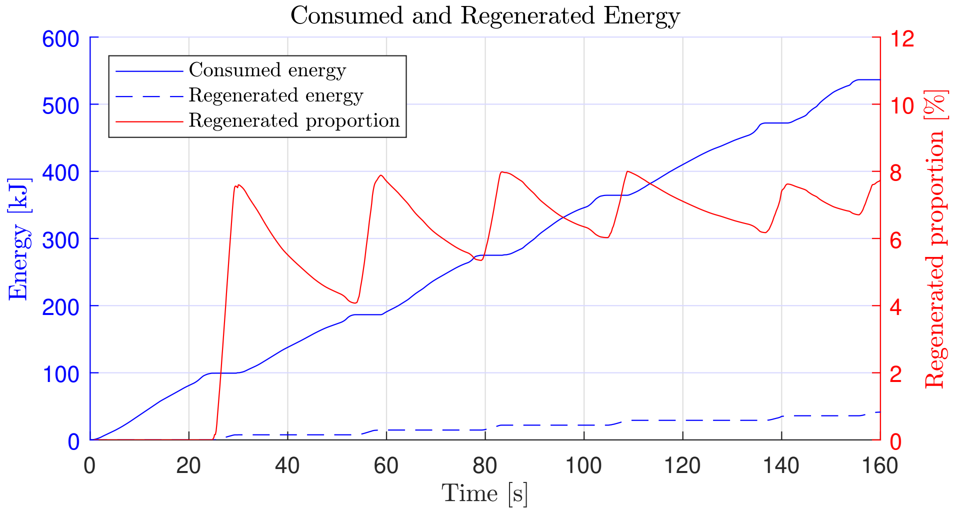

Figure 7.28: Used and regenerated energy for the rig during the grading test. The proportion of regenerated energy compared to used energy.

Chapter 8

Discussion

The results obtained in Chapters 5 and 7 for the original and new system are in this chapter discussed. The reason for these results and the consequences of the used components are evaluated. The used method for comparing the two systems are also questioned and problematised.

8.1 System Design

The used components for the rig are, as mentioned earlier, all chosen in advance from preexisting components. The used components are thus not optimal for this purpose. This is made clear in Section 4.2.1 where the pump displacement setting is limited to 50 % which results in a reduced maximum efficiency. By increasing the size of the boost pump, the maximum displacement setting can be increased resulting in a higher efficiency. With an increased displacement setting the rotational speed will be decreased for the same flow resulting in offsetting the complete speed spectrum for the EMG to operation points with a lower efficiency. A different solution to the maximum displacement setting limitation is to reduce the size of the main pump and have the same size of the boost pump. This will increase the system efficiency but result in difficulties finding a suitable hydraulic machine. All the hydraulic machines in the same product family as the one used, have almost the same ratio between the main and boost pump displacement leading to these being excluded from possible alternatives as hydraulic machine. The used pump is also not manufactured to run as an motor, resulting in the relatively low efficiency during regeneration. With a hydraulic machine that is better suited for this type of system the overall efficiency can be improved.

Since the area compensating flow is only required during extension of the cylinder, the power used by the boost pump is only resulting in losses during retraction. A different system design would be to decouple the area compensating flow source from the main pump and either have an external flow source in terms of further one electric motor and pump that is only active during extension or to use the original system on the Tigon to supply the extra flow when necessary. One aspect that must be taken into account if integrating the area compensating flow into the original system is that the extra flow can result in extra losses due to differences in load pressure. By investigating the pump pressure on the Tigon machine during the excavating and grading test, presented in Figures 7.14 and 7.25, the pressure is fluctuating around 50 bar during the excavating and is almost constant at 30 bar during grading. With a maximum area compensating flow of 23.3 l/min, and the set boost pressure of 25 bar, the resulting throttling pressure drop is up to around 25 bar during excavating. The hydraulic power losses for the area compensating flow due to the differences in load pressure is thus 1.0 kW at worst case. During grading, the throttling pressure drop is only 5 bar resulting in losses under 0.2 kW. The losses also decreases with a lower cylinder velocity. For the used system design, the boost pump rotates at between 500 and 2000 rpm, producing a flow of between 14.2 and 56.6 l/min with a pressure of 25 bar resulting in a hydraulic power losses of 0.6 to 2.4 kW.

With the area compensating flow supplied from the original system, the options increases regarding choice of pump that is better adapted for this type of system. In conclusion, by using the original system as provider for the area compensating flow, the hydraulic machine can be replaced with a machine more suited to run as both a pump and motor, resulting in higher efficiency and lower energy consumption.

To improve the efficiency at low displacement settings, the conventional variable machine can be replaced with a machine with digital displacement. The digital displacement machine is reported to keep the high efficiency even during lower displacement settings which will improve the overall efficiency [21]. By changing the system design and instead using a fixed displacement pump the overall efficiency for the pump can be as high as 95 % for bent-axis machines [22]. This, however, removes the displacement setting as a control variable and thus the possibility of reducing the displacement when the required torque is higher than the maximum torque from the prime mover. This results in a more powerful prime mover might being required depending on the displacement of the fixed displacement pump.

As the system only has a dump valve on Line B and not Line A, the system is not able to regenerate any power if the B line is the high pressure side. The B line is the high pressure side when the bucket, or any other tool, has been pushed downwards into, or onto, the ground. Pressurising the B chamber is only used for applying a pressure on the ground with the attached tool on the backhoe, there is thus no available flow that can be used for regeneration. This is seen in Figure 7.12 where the negative pressures only are short peaks. An extra dump valve on the A line is thus unnecessary. However, as the system is now, it is not possible to control the speed of depressurising of chamber B. This can be solved by replacing the current dump valve consisting of the On/Off and the pressure relief valve with a proportional 2/2 valve. This will give complete control to the operator, which can be used to set a desired pressure in the B chamber. By regulating the pressure in the B chamber, the operator can apply a constant force on the attached tool on the backhoe.

The main disadvantages of implementing a separate system for the boom cylinder is the increase of components which increases the cost of the machine. Another issue is the lack of space in the Huddig Tigon making it more complicated to integrate the new boom cylinder system.

8.2 Characteristics

The characteristics is only tested during a positive load force, i.e. a pulling load on the boom cylinder, for the same reason as not implementing a dump valve on the A line. The amount of flow in to, and out from, cylinder chamber B during negative load force is very limited. The resulting characteristics map is thus used during both negative and positive load.

The validation of the characteristics map in Figure 5.3 made in Section 5.3 shows that the map is correct for higher pressures, but needs some tuning for lower pressures. The used control strategy, that is evaluated in Figures 5.7 and 5.8, proves to be working since the actually measured flow and the requested flow follows the same pattern. The measured flow during higher load and higher demanded flow is though too low. This may indicate that the efficiency map for the pump is not completely accurate at higher pressures. It can also depend on the pressure reducing feed valve in the pump that reduces the displacement setting if the pressure is to high. Since the actual displacement setting can not be measured it is not known if it depends on the efficiency map or the actual displacement setting being altered.

To validate the behaviour of the characteristic on the new system an experienced operator tested the new system and confirmed that the known characteristics were implemented on the new system. Due to the different system design, the new system makes a different noise compared to the original, which was unfamiliar to the operator, resulting in a different impression of the new system.

During the analysis of the characteristics on the original systems and the development of how to achieve this characteristics for the rig, it is assumed that the original system has the desired and optimal characteristic for the boom cylinder. The only way to change the characteristics on the original system is to change the design of the pressure feedback system on the directional valve in the valve manifold. This change is a time-consuming and costly procedure. On the new system, with the electronically controlled characteristics, the pressure feedback can easily be altered and customized, even during operation of the backhoe, depending on the current situation and the desired behaviour.

8.3 Control Strategy

The used control strategy is not an optimal strategy for this kind of system. The reason for choosing the implemented control strategy is due to lack of data on the used components and time limitation. With more available time a control strategy based on the efficiency map in the available data points would have been possible. This would result in greater energy savings than the one presented in Chapter 7. Since the chosen pump is not suitable for this kind of system, more time spent on the control strategy was not prioritised.

With both a variable speed and variable displacement, different control strategies can be implemented to be used at different operations. For example an *ECO* mode that always uses the optimal speed and displacement setting regarding to energy efficiency or an *Optimal Dynamics* mode with higher damping and a higher volume flow gradient available for optimal control.

8.4 Energy Analysis

Since the Huddig machines are used so versatile there are no tests that would represent all different area of use. In order to evaluate the possible energy savings that can be made with the new system compared to the original, three different tests were performed.

When comparing the measurements and the results for the two systems, it should be noted that, since the machine was controlled by a human operator, the motion of the backhoe was not exactly the same for the two systems. A different approach would have been to implement a predefined motion in the control system to get a more reliable comparison of the two systems. However, by comparing the position of the bucket, cylinder stroke, and boom cylinder pressure for the two systems during the measurements they are considered to be sufficiently equal to give a comparable result.

The first test analyses the energy recovery capacity while lifting and lowering the boom at a constant speed for a certain backhoe position and bucket weight. This test gives an outline of the amount of energy used for lifting the backhoe that can be regenerated back into the battery during lowering. Under optimum conditions the rig can regenerate up to 19 % at optimal flow during lifting and lowering. This is however not the case during actual operation, since normal operation often includes loading and unloading loads at different heights and might not operate at optimal flows. As seen in Figures 7.19 and 7.28, the proportion of regenerated energy during the excavating and grading operation is between 7 and 8 % of the used energy.

The energy savings are however greater. During both the excavating and grading test the new system used 30 % less energy. The operational time will be extended with more than 40 % with the new system as it is today. With a better suited components and a better control strategy, the energy savings can be increased even further. A simple improvement is to replace the LHV to one with a lower pressure drop. The required energy to lift the boom will be decreased and the regained hydraulic energy will be increased. As seen in Figure 7.7, the hydraulic efficiency reduces with a higher flow rate. The increased losses is due to the higher pressure drop across the LHV illustrated in Figure 4.9. By replacing the LHV the positive slopes on the dashed lines in Figures 7.16 and 7.26 will be decreased and the negative slope will be increased resulting in a lower net use of energy from the rig for the new system.

By comparing the rig to the closest comparable systems in [2] the energy saving of approximately 50 % illustrated in Figure 7.8 are believed to be able to be further increased to 75 % of the original system.

Chapter 9

Conclusion

This chapter summarizes the thesis and presents the conclusions made as answers to the research questions asked in Section 1.2. For further improvements of the new system, some future work is also proposed in this chapter.

9.1 Summary

Pump-controlled hydraulic system is an ongoing research area which has shown great potential in several studies, which has also been demonstrated in this thesis. This thesis shows the potential of energy savings on a pump-controlled hydraulic system with a simple external rig. With the used components energy savings of 30 % was proven for both low and high energy demanding operations. With better suited components and further development of the system, energy savings of over 50 % is believed to be possible.

With lower energy consumption, longer operating times are possible with a battery of the same capacity. With a lower energy consumption and a longer operating time, the incentive to switch to electrical hybrid machines and pump-controlled systems increases within earth-moving machinery and load handling machines. With a lower energy consumption, the operating cost is decreased and the human impact on the environment is reduced. With further research and development, pump-controlled systems are believed to be a part of the backhoe loaders, excavators and load-handling machines in the future.

9.2 Answers to the Research Questions

How can the existing characteristics of the backhoe be measured and defined?

The existing characteristics of the boom cylinder is defined by the relationship between the operator reference signal, the cylinder pressure and the cylinder flow. The defined characteristic in Figure 5.3 proved to be accurate for higher pressures during both positive and negative flow seen in Figure 5.6. During the light load the characteristics map needs to be reviewed for positive flow.

How can a similar characteristic of the backhoe with the new system be achieved?
Similar characteristics for the new system is achieved by using the volumetric efficiency of the pump to predict the output flow from the pump at certain pump pressures, displacement setting and rotational speeds. This strategy is verified by Figures 5.7 and 5.8, where the requested flow and the actual flow are compared. This strategy is proven to function for all different flows at lower loads and for all except high flow demands at a high pressure load. At higher flow demand and higher pressures, the measured flow does not reach the requested flow, but it follows the same pattern of the requested flow.

To what extent is it possible to regenerate energy from the boom cylinder on a backhoe?
During pure regeneration from potential to electric energy regenerated back into the battery the rig as an efficiency of up to 39 % during the investigated tests. For a lifting and lowering cycle with the same load up and down, as tested in the energy recovery test, the rig has an over all recovery efficiency of up to 19 %. During the excavation and grading tests, where complete cycles are analysed, an energy regeneration of approximately 8 % of the used energy for both tests are achieved. By using a better suited pump, a LHV with a lower pressure drop and a control strategy derived from complete efficiency maps of the components the efficiency during regeneration is considered to be able to be increased substantially.

How much energy savings can be expected with the new system compared to the original system?
With the use of regeneration and the sectioning of the hydraulic system, energy savings of 30 % for the complete system was achieved during both excavation and grading. With a reduced energy consumption of 30 %, the operation time is increased with over 40 %. With better suited components and a more advanced control strategy, energy savings of over 50 % is thought to be possible, which will increase the operation time by 100 % compared to the original system.

Are the chosen components suitable for this type of system or how can they be improved or replaced?
The used hydraulic pump is oversized for this purpose of only being used to supply one cylinder. The pump can be replaced with a smaller more suitable pump for this type of system. The area compensating flow can be supplied from a separate pump or the original system through a pressure reducing valve resulting in a system with higher efficiency and the energy savings can be increased. A pump where the displacement setting can be measured will also give more information back to the system to verify the output flow of the pump. With a different pump, the EMG might has to be changed, depending on the displacement, minimum and maximum speed of the chosen pump.

To increase the regeneration efficiency, the LHV should be replaced with a valve with a lower pressure drop. As seen in Figure 7.7b the hydraulic losses is almost 40 % during higher flows. These losses can almost be completely eliminated by exchanging the LHV.

The used On/Off valve in the dump valve depressurises the cylinders B chamber directly to approximately 25 bar. This valve should be replaced with a proportional valve giving a better control of the depressurising.

9.3 Future Work

Since this is a study based on a simple prototype with components not suited for this type of system, there is a lot of room for improvements. This section presents some of these improvements that is believed to have the highest potential to reduce the energy consumption even further and the ability to improve the controlability of the new system.

- The hydraulic machine is, as stated previously, oversized for this type of system. A suggestion is to use a better suited hydraulic machine with a smaller displacement, and to use the original system as flow source for the area compensation flow. A hydraulic machine with a measurable displacement setting will also improve the ability to predict the flow output from the pump.

- For better control of the boom cylinder during negative load force, the used dump valve should be replaced with a valve with higher controllability.

- As mentioned in Section 5.3, the characteristics map in Figure 5.3 needs to be improved for some load cases.

- The implemented control strategy has a lot of potential for improvements. It does not utilise all the advantages of having both a variable speed and variable displacement. With these two degrees of freedom it is possible to develop different control strategies for different types of operation. Whether it is desirable to be able to choose between different control strategies or not is something that should be investigated further.

- It is demonstrated that the losses due to differences in load pressure is the source of substantial losses in the valve-controlled system. Even if implementing a separate system for the boom cylinder, there will still be losses due to different load pressures among the remaining cylinders. To reduce these losses the pressure in the different cylinders should be investigated for different load cases. By changing the cylinder area, the required load pressures can be altered to better match between the different cylinders and the losses can be reduced.

Bibliography

[1] P. Bogatir, "Industriell kreativitet i gummistövlar", *Hydraulikguiden*, pp. 22–23, 2020.

[2] S. Ketelsen, D. Padovani, T. O. Andersen, M. K. Ebbesen, and L. Schmidt, "Classification and review of pump-controlled differential cylinder drives", *Energies*, vol. 12, no. 7, p. 1293, 2019.

[3] J. Willkomm, M. Wahler, and J. Weber, "Potentials of speed and displacement variable pumps in hydraulic applications", in *Proceedings of the 10th International Fluid Power Conference, Dresden, Germany*, 2016, pp. 8–10.

[4] A. Imam, M. Rafiq, E. Jalayeri, and N. Sepehri, "Design, implementation and evaluation of a pump-controlled circuit for single rod actuators", in *Actuators*, Multidisciplinary Digital Publishing Institute, vol. 6, 2017, p. 10.

[5] T. A. Minav, L. I. Laurila, and J. J. Pyrhönen, "Analysis of electro-hydraulic lifting system's energy efficiency with direct electric drive pump control", *Automation in construction*, vol. 30, pp. 144–150, 2013.

[6] Z. Quan, L. Quan, and J. Zhang, "Review of energy efficient direct pump controlled cylinder electro-hydraulic technology", *Renewable and Sustainable Energy Reviews*, vol. 35, pp. 336–346, 2014.

[7] M. Axin, "Mobile working hydraulic system dynamics", PhD thesis, 2015.

[8] J. Willkomm, M. Wahler, and J. Weber, "Model predictive control of speed-variable variable-displacement pumps to optimize energy efficiency", in *9th International Fluid Power Conference, Aachen*, vol. 1, 2014, pp. 372–385.

[9] A. Imam, M. Rafiq, T. Zeljko, and N. Sepehri, "Improving the performance of pump-controlled circuits for single-rod actuators", in *Actuators*, Multidisciplinary Digital Publishing Institute, vol. 8, 2019, p. 26.

[10] J. Edén and F. Lagerstedt, "An electro-hydraulically controlled cylinder on a loader crane", Master's thesis, Linköping University, 2018.

[11] Huddig. (2020). Customer cases, [Online]. Available: `https://www.huddig.com/products/customer-cases/` (visited on 04/09/2020).

[12] G. Altare and A. Vacca, "A design solution for efficient and compact electro-hydraulic actuators", *Procedia Engineering*, vol. 106, pp. 8–16, 2015.

[13] *Global Vehicle Motors GVM Series, Technical Manual*, 20-02-10 PVD 3668_GB GVM February 20, Parker, 2018.

[14] Empowering. (2017). Customer cases, [Online]. Available: `https://empoweringpumps.com/ac-induction-motors-versus-permanent-magnet-synchronous-motors-fuji/` (visited on 04/12/2020).

[15] R. Bansal, *A textbook of fluid mechanics and hydraulic machines*. Laxmi publications, 2004.

[16] *Axial piston variable pump - A4VG Series 32*, RE 92003-01-B/12.2015, Bosch Rexroth, 2015.

[17] *Axial piston variable pump - A4VG Series 32*, RE-E 92003/06.2018, Bosch Rexroth, 2018.

[18] "ISO 8643: Earth-moving machinery — Hydraulic excavator and backhoe loader lowering control device — Requirements and tests", International Organization for Standardization, Standard, 2017-02.

[19] *IQAN-MC4x, -XC4x Instruction book*, Parker, 2019. [Online]. Available: `https://www.parker.com/Literature/Electronic%20Controls%20Division/Literature%20files/IQAN-MC4x_XC4x_MSG17-8413-IB_UK.pdf` (visited on 04/12/2020).

[20] *K170ls mobile directional control valve*, Parker, 2010. [Online]. Available: `https://www.parker.com/literature/Mobile%20Controls%20-%20Europe/HY17-8557-SE_K170.pdf` (visited on 04/21/2020).

[21] J. J. Budden and C. Williamson, "Danfoss digital displacement® excavator: Test results and analysis", in *Fluid Power Systems Technology*, American Society of Mechanical Engineers, vol. 59339, 2019, V001T01A032.

[22] *Hydraulic Motor/Pump, Series F11/F12, Fixed Displacement*, MSG30-8249/SE, Parker, 2019.

Appendix A

Mechanic Calculations

To be able to calculate the potential energy and power of the lifted or lowered load the backhoe mechanics is designed in MATLAB*. This appendix explains how these calculations has been implemented and how the potential energy and power is calculated.*

A.1 Backhoe Points of Interest

All joints between the different components of the backhoe is essential to be able to copy the mechanics of the backhoe, these points are illustrated and named in Figure A.1. A global coordinate system is also essential to describe each joints

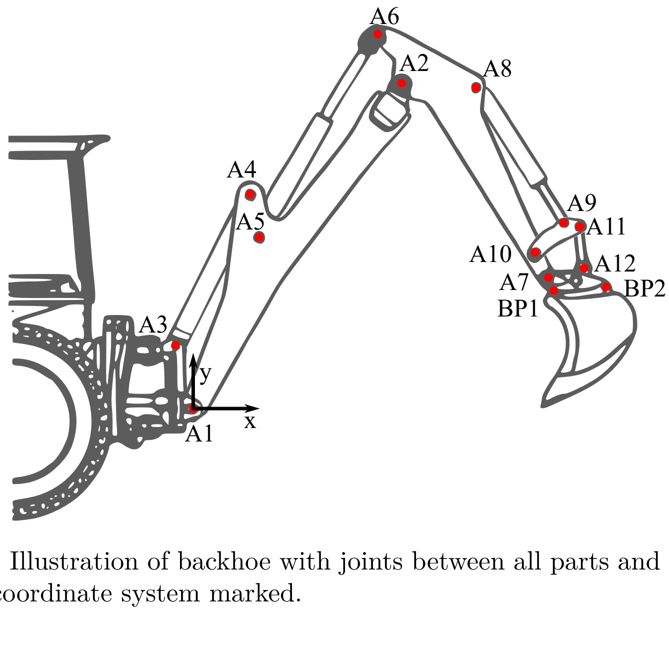

Figure A.1: Illustration of backhoe with joints between all parts and the origin of the global coordinate system marked.

location. The global coordinate systems is fixed and does not move or rotate when moving the boom, dipper or bucket cylinder. The origin of the global coordinate system is set in point A1 and the x-axis is parallel to the ground and the y-axis is perpendicular to the ground, illustrated in Figures A.1 and A.2. A description of the joints is presented in Table A.1.

Table A.1: Description of points in Figure A.1.

Point	**Description**
A1	Joint between Swing post and Boom.
A2	Joint between Boom and Dipper.
A3	Joint between Swing post and Boom cylinder
A4	Joint between Boom cylinder and Boom
A5	Joint between Boom and Dipper cylinder
A6	Joint between Dipper cylinder and Dipper
A7	Joint between Dipper and the Quick coupler
A8	Joint between Dipper and Bucket cylinder
A9	Joint between Bucket cylinder and Link rod 1
A10	Joint between Dipper and Link rod 1
A11	Joint between Link rod 1 and Link rod 2
A12	Joint between Link rod 2 and Quick coupler
BP1	Joint between Quick coupler and Bucket
BP2	Joint between Quick coupler and Bucket

To calculate the potential energy of the backhoe the mass and CoG for all major components are required. The CoG for each component is illustrated in Figure A.2 with their respective name.

Table A.2: Description of points in Figure A.2.

Point	**Description**
B1	CoG Boom
B2	CoG Dipper
C1	CoG Boom cylinder
C2	CoG Dipper cylinder
C3	CoG Bucket cylinder
C4	CoG Side-angling cylinder
EL	CoG Side-angling link
KL	CoG Knot link
L1	CoG Link 1
L2	CoG Link 2
L3	CoG Quick coupler
Bucket	CoG Bucket

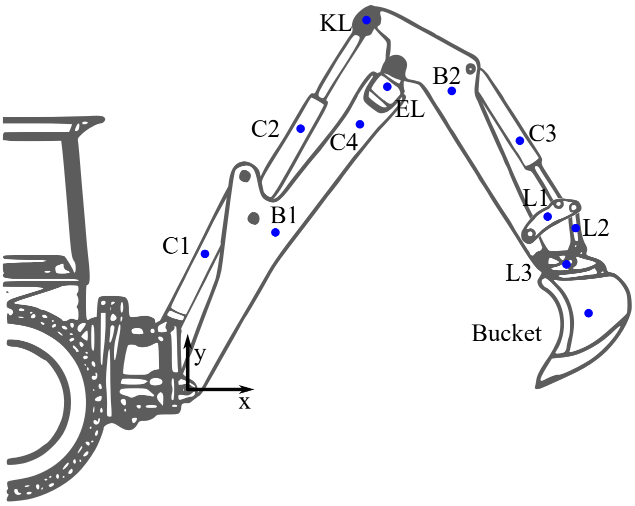

Figure A.2: Illustration of backhoe with points representing the CoG for respective part. Note that point C4 is the CoG for the Side-angling cylinder which is not included in the figure.

A.2 Trigonometry

With point A1 and A3 fixed in the global coordinate system, the remaining points can be calculated in relation to these points. The distant between all points on one component is known and the length of the cylinders is measured with linear length transducers during all measurements. By making a triangle with two known points, one unknown as all distances between the points known as illustrated in Figure A.3, the unknown point can be calculated using the law of cosine in Equation (A.1).

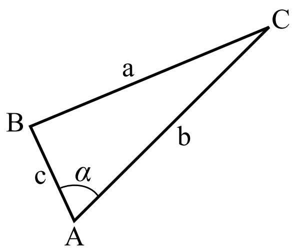

Figure A.3: Triangle with notation for the law of cosines in Equation (A.1). Point A and B are known points and point C is unknown. All lengths, a, b, and c are known.

$$\alpha = \arccos \frac{b^2 + c^2 - a^2}{2bc} \tag{A.1}$$

With the A and B points known the global angle of line AB are known and with the local angle α remaining angles can be calculated. Point C can now be calculated using trigonometric functions.

A.3 Kinematic Calculation

This section describes how the points of interest in Figures A.1 and A.2 are calculated.

Fixed Joints, A1 and A3

Point A1 and A3 are always fixed in the global coordinate system and does not depend on the length of the cylinders.

Joint A4

Joint A4 is the connection between Boom and Boom cylinder. Since point A1 and A3 are known in the global coordinate system the angle θ_3, in Figure A.4, can be calculated using Equation (A.2). The point A4 can be calculated by forming a triangle, illustrated in Figure A.4, with A1 and A3 where all lengths are known. The angle α_4 is calculated using the law of cosines in Equation (A.1). α_4 together with the global angle θ_3 is used to calculate the global angle θ_4 in Equation (A.3).

$$\theta_3 = \arctan\left(\frac{A1_x - A3_x}{A1_y - A3_y}\right) + \pi/2 \tag{A.2}$$

$$\theta_4 = \theta_3 - \alpha_4 \tag{A.3}$$

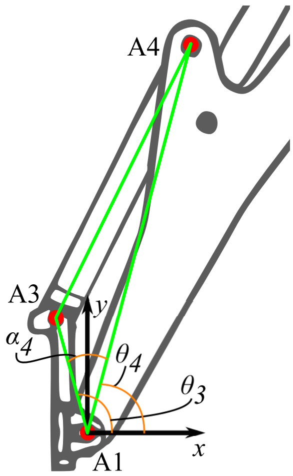

Figure A.4: Illustration of how the coordinates of point A4 are calculated.

With the length between point A1 and A4 together with the global angle θ_4 the x and y coordinate for point A4 is given by Equation (A.4).

$$A4 = \begin{bmatrix} A4_x \\ A4_y \end{bmatrix} = \begin{bmatrix} A1_x + A1A4 \cdot \cos\theta_4 \\ A1_y + A1A4 \cdot \sin\theta_4 \end{bmatrix} \tag{A.4}$$

A.3.1 Remaining Joints

All other joints, including the CoG points, are calculated using the approach described in Appendix A.3. By making a triangle with two known joints and one unknown where all lengths are given all joints on the backhoe can be calculated.

A.4 Center of Gravity

The x coordinate of the global CoG is calculated using Equation (A.5) where $l_{x,k}$ is the horizontal distance between the global origin in A1 and the CoG of component k and n is the total number of components.

$$x_{CoG} = \frac{\sum\limits_{k=1}^{n} l_{x,k} m_k}{m_{tot}} \tag{A.5}$$

The vertical position, i.e. the y coordinate, of the CoG is calculated using Equation (A.6)

$$y_{CoG} = \frac{\sum\limits_{k=1}^{n} l_{y,k} m_k}{m_{tot}} \tag{A.6}$$

A.5 Torque Equilibrium

Torque equilibrium is used to calculate the force acting on boom cylinder in steady state, i.e. no acceleration is included in the calculations, Equation (A.7). The tests where the potential energy is used for analysis the tests are performed to fulfill this simplification as much as possible.

$$\sum T = 0 \tag{A.7}$$

The CoG and the total calculated mass of the backhoe is used according to the free body diagram in Figure A.5 to calculate the force acting on boom cylinder using Equations (A.8) and (A.9).

$$\overset{\frown}{A1}: \; F_{CoG} x_{CoG} - F_{cyl1} l_{cyl1} = 0 \tag{A.8}$$

$$F_{cyl1} = \frac{F_{CoG} x_{CoG}}{l_{cyl1}} \tag{A.9}$$

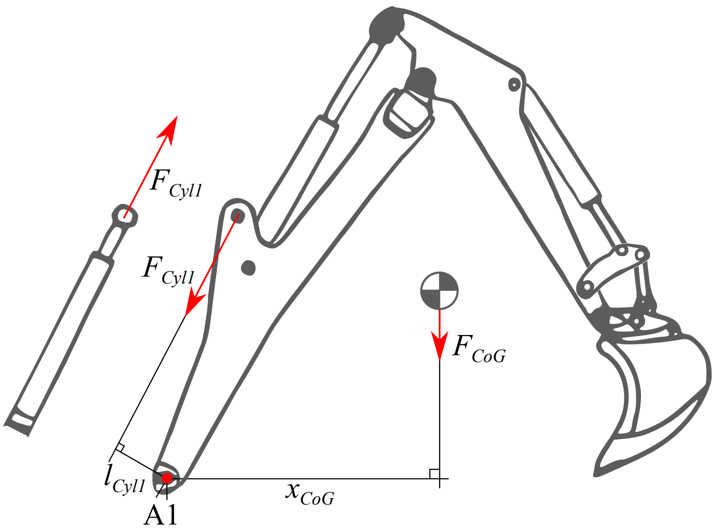

Figure A.5: Free body diagram of the boom cylinder and the backhoe.

A.6 Validation

To validate the mechanic model the actual load force is calculated by measuring of the pressures in chamber A and B on the boom cylinder during a random operation and using Equation (A.10).

$$F_{load} = F_A - F_B = p_A A_A - p_B A_B; \tag{A.10}$$

The stroke lengths from the measured operation is used in the mechanic model to calculate the models load force acting on the cylinder. By comparing the measured load force with the calculated from the mechanic model the model can be validated. This comparison is illustrated in Figure A.6. The mechanic model has an constant offset. By taking the average ratio between the measured and calculated force a quotient of 1.19 is obtained. This quotient represents all non included parts in the mechanic model, which is all hoses, bolts and nuts, axis and miscellaneous.

To validate the model, another measurement is performed. By taking the cylinder strokes from the new measurement the mechanic model can calculate the new load force but with an increased total mass, m_{tot}, of the backhoe by 19 %. The measured load force with the calculated from the mechanic model with the increased total mass is illustrated in Figure A.7. As seen in the figure, the measured load force and the calculated from the mechanic model coincide with each other validating the mechanic model.

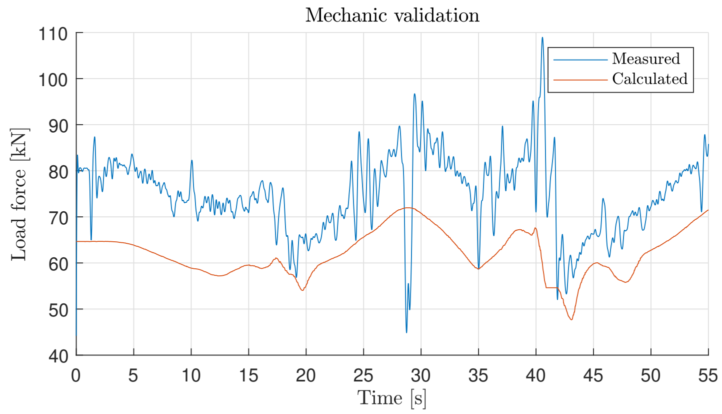

Figure A.6: Measured and calculated load force for the boom cylinder.

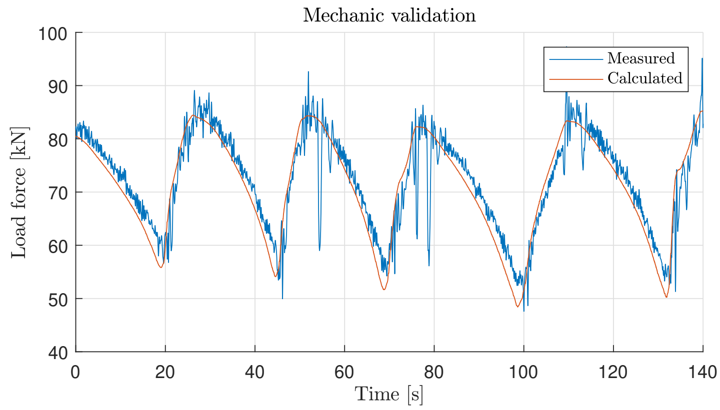

Figure A.7: Validation of the mechanic model with compensated backhoe mass.

A.7 Potential Energy and Power

To calculate the increased or decreased potential power and energy of the backhoe the backhoes CoG is used. The location of the CoG is calculated as described above and the total mass of the backhoe is increased with 19 % to compensate for not included parts of the backhoe as described in the validation for the mechanic model.

With the vertical speed of the CoG, $\frac{dy}{dt}$ known the potential power is calculated using Equation (A.11) and the gained or lossed potential energy is calculated using Equation (A.12).

$$P_{pot} = m_{tot}\ g \frac{dy}{dt} \tag{A.11}$$

$$E = P\ dt \tag{A.12}$$